MITP/16-092
MIT-CTP-4832

Impeded Dark Matter

Joachim Kopp,[1,*] Jia Liu,[1,†] Tracy R. Slatyer,[2,‡] Xiao-Ping Wang,[1,§] and Wei Xue[2,¶]

[1] *PRISMA Cluster of Excellence & Mainz Institute for Theoretical Physics, Johannes Gutenberg University, Staudingerweg 7, 55099 Mainz, Germany*

[2] *Center for Theoretical Physics, Massachusetts Institute of Technology, Cambridge, MA 02139, USA*

(Dated: December 15, 2016)

We consider dark matter models in which the mass splitting between the dark matter particles and their annihilation products is tiny. Compared to the previously proposed Forbidden Dark Matter scenario, the mass splittings we consider are much smaller, and are allowed to be either positive or negative. To emphasize this modification, we dub our scenario "Impeded Dark Matter". We demonstrate that Impeded Dark Matter can be easily realized without requiring tuning of model parameters. For negative mass splitting, we demonstrate that the annihilation cross-section for Impeded Dark Matter depends linearly on the dark matter velocity or may even be kinematically forbidden, making this scenario almost insensitive to constraints from the cosmic microwave background and from observations of dwarf galaxies. Accordingly, it may be possible for Impeded Dark Matter to yield observable signals in clusters or the Galactic center, with no corresponding signal in dwarfs. For positive mass splitting, we show that the annihilation cross-section is suppressed by the small mass splitting, which helps light dark matter to survive increasingly stringent constraints from indirect searches. As specific realizations for Impeded Dark Matter, we introduce a model of vector dark matter from a hidden $SU(2)$ sector, and a composite dark matter scenario based on a QCD-like dark sector.

arXiv:1609.02147v3 [hep-ph] 14 Dec 2016

* jkopp@uni-mainz.de
† liuj@uni-mainz.de
‡ tslatyer@mit.edu
§ xiaowang@uni-mainz.de
¶ weixue@mit.edu

CONTENTS

I. Introduction 2

II. Dark SU(2) Gauge Bosons as Impeded DM with $\Delta < 0$ 4
II.1. Model 4
II.2. Relic Density 6
II.3. Direct Detection 8
II.4. Constraints from the Cosmic Microwave Background 11
II.5. Indirect Detection 12

III. Dark Pions as Impeded DM with $\Delta > 0$ 14
III.1. Model 14
III.2. Constraints from relic abundance, direct and indirect detection 16

IV. Conclusions 18

Acknowledgments 19

A. DM annihilation to SM particles in the $SU(2)_d$ model 19

B. K_3 decay to SM particles in the $SU(2)_d$ model 20

References 21

I. INTRODUCTION

Many theories in particle physics live through an infancy in which they are carved out by a few pioneering masterminds, a youth characterized by wild enthusiasm in the broader community, an adulthood in which they become part of university curricula, and the sunset years during which lack of experimental evidence leads to disillusionment or at least fatigue in the community. Models of Weakly Interacting Massive Particles (WIMPs) may be approaching this last stage of their life cycle and may eventually fade away unless solid experimental evidence for WIMP dark matter (DM) is discovered soon. Nevertheless, this time has not come yet, and in fact WIMPs are experiencing an Indian summer with fresh ideas and models sprouting from the arXiv on a regular basis. Promising recent developments include Secluded DM [1, 2], SIMP [3–6], Selfish DM [7], Forbidden DM [8, 9], Cannibal DM [10–15], Co-decaying DM [16–18], Semi-annihilating DM [19], Boosted DM [20–22], and DM with late-time dilution [23]. These scenarios are characterized by a dark matter sector with non-minimal particle content and interesting, unconventional dynamics.

This is also true for the scenarios we wish to consider in the present work. In particular, we consider situations in which the dynamics of DM in the early Universe is governed by a dominant annihilation channel $\mathrm{DM\,DM} \to \mathrm{X\,X}$, with the special feature that the mass splitting $\Delta \equiv m_{\mathrm{DM}} - m_{\mathrm{X}}$ between DM and X is very small, $|\Delta| \ll m_{\mathrm{DM}}$. Our scenario is thus closely related to Forbidden DM [8, 9] and Co-decaying DM [16–18]. We allow Δ to be either positive or negative, and we assume that X couples also to SM particles. The dynamics of DM annihilation in the non-relativistic regime is governed by the phase space factor in the cross-section, therefore we call this scenario "Impeded Dark Matter". Explicitly, the velocity-averaged annihilation cross-section for Impeded DM has the

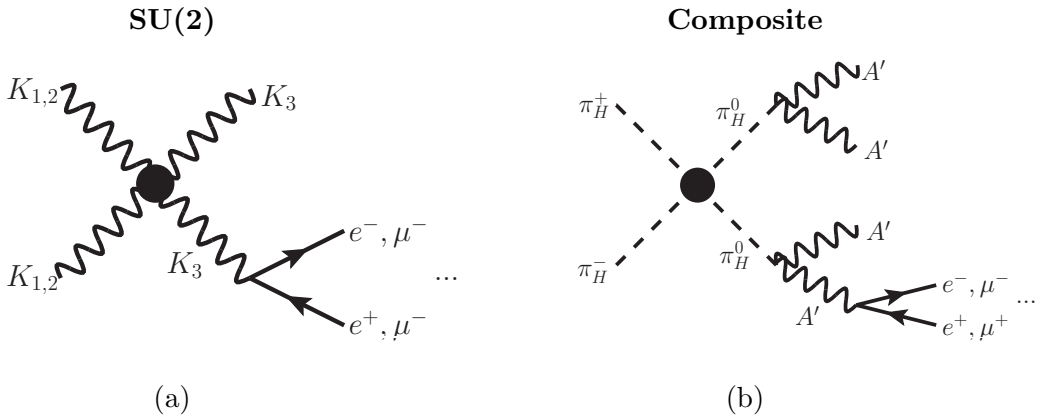

Figure 1. Dark matter annihilation in two Impeded DM models: (a) a dark $SU(2)$ model with $\Delta \equiv m_{\rm DM} - m_{\rm X} < 0$, where $K_{1,2,3}$ are the gauge bosons associated with the new gauge symmetry. K_1 and K_2 are degenerate in mass, while K_3 is slightly heavier thanks to a higher-dimensional coupling. The same coupling also mixes K_3 with the SM hypercharge boson B. (b) a QCD+QED-like composite dark sector with $\Delta > 0$, in which the mass-degenerate charged dark pions $\pi_H^\pm$ act as the dark matter, while their neutral partner π_H^0 can decay to two dark photons A' through the chiral anomaly.

form (see also [24])

$$\langle \sigma v_{\rm rel} \rangle = \int \frac{d\sigma_0}{d\Omega} \frac{1}{4\pi} \sqrt{1 - \frac{4m_{\rm X}^2}{s}} d\Omega \;\simeq\; \sigma_0 \sqrt{\frac{v_{\rm rel}^2}{4} + \frac{2\Delta}{m_{\rm DM}}} \,. \tag{1}$$

We consider only scenarios in which σ_0 is independent of $v_{\rm rel}$ at leading order, i.e. in which DM annihilation is an s-wave process. Around the time of DM freeze-out, when $\langle v_{\rm rel}^2 \rangle \sim 0.26$ is large enough to neglect the mass difference Δ, but low enough to treat DM and X as non-relativistic, we obtain $\langle \sigma v_{\rm rel} \rangle \simeq \sigma_0 v_{\rm rel}/2$. This linear dependence on $v_{\rm rel}$ distinguishes Impeded DM from most other DM models, in which $\langle \sigma v_{\rm rel} \rangle$ is either velocity-independent or proportional to $v_{\rm rel}^2$. (Scenarios where phase space suppression leads to a linear dependence of $\langle \sigma v_{\rm rel} \rangle$ on $v_{\rm rel}$ have also been discussed recently for instance in refs. [16, 17, 24].)

From a theorist's point of view, the small mass splitting Δ can be explained easily, for instance if the DM and X are members of the same multiplet under a gauge symmetry, global symmetry, or supersymmetry (SUSY). Once the symmetry is broken by a small amount—as is desirable to allow X to decay to SM particles—$m_{\rm DM}$ and $m_{\rm X}$ become split, either at tree level or through loop effects. In the following, we investigate in particular small mass splittings arising from a dark sector gauge symmetry $SU(2)_d$, or from an approximate global chiral symmetry in a composite hidden sector. The annihilation processes for both cases are illustrated in fig. 1. We will not discuss SUSY here, but we remark that Impeded DM can be easily realized in stealth SUSY [25–27] under the condition that Δ is larger than the gravitino mass.

We summarize the main phenomenological features that distinguish Impeded DM models from other scenarios.

- The linear dependence of the annihilation cross-section on the DM velocity is crucial for indirect detection: it leads to strong signals in regions of larger DM velocity such as galaxy clusters or the Galactic center, while signals from objects with low DM velocity dispersion, in particular dwarf galaxies, are suppressed.

- If $\Delta < 0$ (DM lighter than X), annihilation to XX becomes kinematically forbidden at too low DM velocity. This is phenomenologically relevant when $\langle v_{\rm rel}^2 \rangle < 8|\Delta|/m_{\rm DM}$, in which case the cross-section $\langle \sigma v_{\rm rel} \rangle$ is Boltzmann suppressed. Typical values for $\langle v_{\rm rel}^2 \rangle$ are 10^{-9} in dwarf galaxies, 10^{-6} in the Milky Way, 10^{-5} in galaxy clusters, 0.26 at freeze-out, and $< 10^{-9}\,{\rm GeV}/m_{\rm DM}$ at the epoch of last scattering relevant to the CMB limits.[1]

- For $\Delta > 0$, the parametric dependence of the annihilation cross-section changes at very low velocity, making $\langle \sigma v_{\rm rel} \rangle$ dominated by the mass splitting and independent of $v_{\rm rel}$. DM annihilation is never kinematically forbidden in this case.

The remainder of this paper is organized as follows: In section II, we introduce a dark $SU(2)$ model as a promising example for Impeded DM with $\Delta < 0$. The setup of this model is discussed in section II.1. We calculate the relic abundance in section II.2, and discuss the direct detection, CMB and indirect constraints in section II.3, section II.4 and section II.5 respectively. As an example for $\Delta > 0$, we then study a dark pion model in section III. Once again, we commence by introducing the model in section III.1, and then investigate its freeze-out dynamics and detection prospects in section III.2. In section IV, we conclude.

II. DARK SU(2) GAUGE BOSONS AS IMPEDED DM WITH $\Delta < 0$

II.1. Model

Impeded Dark Matter is realized most easily when the DM particle and its annihilation partner are members of the same multiplet under a symmetry group, so that, for unbroken symmetry, their masses are exactly equal. Let us consider in particular a dark sector governed by a dark $SU(2)_d$ symmetry, with the associated gauge bosons accounting for the DM and its annihilation products. $SU(2)_d$ is broken by a scalar doublet $\Phi = (G^1 + iG^2, (v_d + \phi)/\sqrt{2} + iG^3)$, where, G^1, G^2, G^3 are Goldstone bosons, $v_d = 2\sqrt{\langle \Phi^\dagger \Phi \rangle}$ is the vacuum expectation value (vev), and ϕ is a physical dark Higgs boson. The dark sector Lagrangian is then,

$$\mathcal{L} = -\frac{1}{4} K^a_{\mu\nu} K^a_{\mu\nu} + (D_\mu \Phi)^\dagger (D_\mu \Phi) - V(\Phi)\,, \tag{2}$$

with the potential

$$V(\Phi) \equiv -\mu^2 \Phi^\dagger \Phi + \frac{\lambda}{2} (\Phi^\dagger \Phi)^2 \tag{3}$$

and the field strength tensor $K^a_{\mu\nu} = \partial_\mu K^a_\nu - \partial_\nu K^a_\mu + g_d \varepsilon^{abc} K^b_\mu K^c_\nu$, where g_d is the $SU(2)_d$ coupling constant. The three $SU(2)_d$ gauge fields K^1_μ, K^2_μ and K^3_μ initially obtain equal masses

$$m_k = \frac{g_d v_d}{2} \tag{4}$$

due to a residual global $SO(3)$ symmetry.

A dark sector with gauge boson DM can couple to the SM in various different ways. In most models considered in the literature, the dark and visible sectors are connected through Higgs portal interactions [28–41]. Some models instead feature particles from the dark or visible sector that are

[1] If kinetic decoupling between the dark and visible sectors occurs before the epoch of last scattering, as is usually the case, the DM temperature will be even smaller. The reason is that, after kinetic decoupling, the dark sector temperatures evolves as $a^{-2}(t)$, which the photon temperature drops only as $a^{-1}(t)$, where $a(t)$ is the scale factor of the Universe.

charged under both SM and hidden gauge symmetries [42–45], use Abelian kinetic mixing between a hidden $U(1)'$ gauge boson and the SM hypercharge boson B^μ [46], or invoke loop processes and higher dimensional operators [16, 47] to connect the two sectors. In order to avoid introducing extra particles, we will here consider only the renormalizable Higgs portal interaction

$$\mathcal{L}_{\text{Higgs portal}} \equiv \lambda_p(\Phi^\dagger\Phi)(H^\dagger H)\,, \tag{5}$$

and non-Abelian kinetic mixing of the form

$$\mathcal{L}_{\text{mix}} = \frac{1}{\Lambda^2}(\Phi^\dagger T^a \Phi)K^a_{\mu\nu}B_{\mu\nu} \tag{6}$$

at the non-renormalizable level.[2] Here, $B_{\mu\nu}$ is the field strength tensor of SM hypercharge. Non-Abelian kinetic mixing allows K_3 to couple to, and decay into, SM particles. The operator in eq. (6) could arise for instance from a box loop involving heavy vector-like $SU(2)_d$ doublet fermions charged under SM hypercharge and another $SU(2)_d$ singlet heavy fermion carrying the same SM hypercharge.

We will assume kinetic mixing between ϕ and the SM Higgs boson h (eq. (5)) to be small compared to the mixing between gauge bosons from eq. (6). As long as $m_\phi > 2m_k$, an assumption we will make in the following, eq. (5) is not needed to allow ϕ to decay. Instead, the dominant ϕ decay will be $\phi \to K_i K_i$ $(i = 1, 2, 3)$.

After $SU(2)_d$ breaking, the non-Abelian kinetic mixing term takes the form

$$\mathcal{L}_{\text{mix}} \supset \frac{\varepsilon}{2}\left(1+\frac{\phi}{v_d}\right)^2\left[\partial_\mu K^3_\nu - \partial_\nu K^3_\mu + g_d(K^1_\mu K^2_\nu - K^2_\mu K^1_\nu)\right]\frac{1}{\cos\theta_w}B_{\mu\nu}\,, \tag{7}$$

with $\varepsilon \equiv -v_d^2\cos\theta_w/(2\Lambda^2)$, where θ_w is the Weinberg angle. We see that mixing affects the kinetic terms of K^3_μ and B_μ, while $K^{1,2}_\mu$ are unaffected. To move to the physical field basis, we redefine

$$\begin{aligned} K^3_\mu &\to \frac{1}{\sqrt{1-\frac{1}{4}\frac{\varepsilon^2}{\cos^2\theta_w}}}K^3_\mu \\ B_\mu &\to B_\mu - \frac{\varepsilon}{\cos\theta_w}\frac{1}{2\sqrt{1-\frac{1}{4}\frac{\varepsilon^2}{\cos^2\theta_w}}}K^3_\mu \end{aligned}\,, \tag{8}$$

thus removing kinetic mixing and properly normalizing the kinetic terms. We then apply a unitary transformation to diagonalize the gauge boson mass matrix. Henceforth, we will use the notation K^3_μ, Z_μ and A_μ to refer to the *physical* neutral gauge bosons. The mass of the physical K^3_μ is shifted by a term proportional to ε^2 relative to eq. (4):

$$m^2_{K_3} = (m_k - \Delta)^2 = m_k^2\left(1+\frac{\varepsilon^2}{\cos^2\theta_w}\frac{(m_k^2 - \cos^2\theta_w m^2_{Z,\text{SM}})}{m_k^2 - m^2_{Z,\text{SM}}}\right), \tag{9}$$

and thus

$$\Delta \equiv m_k - m_{K_3} \simeq -\frac{m_k}{2}\frac{\varepsilon^2}{\cos^2\theta_w}\frac{(m_k^2 - \cos^2\theta_w m^2_{Z,\text{SM}})}{m_k^2 - m^2_{Z,\text{SM}}} \tag{10}$$

[2] Other operators like $\frac{1}{\Lambda^2}(\Phi^\dagger D^\mu\Phi)(H^\dagger D_\mu H)$ can also contribute to mixing [16], but if the heavy fermions generating eq. (6) do not carry $SU(2)_L$ quantum numbers, these operators will not be generated.

In this expression, θ_w is the weak mixing angle in the $\varepsilon \to 0$ limit and $m_{Z,\mathrm{SM}}$ is the Z boson mass in that limit. We see that $\Delta > 0$ is possible only in a narrow mass window in which $m_{W,\mathrm{SM}} < m_k < m_{Z,\mathrm{SM}}$. For $\varepsilon \neq 0$, the Z boson mass is shifted to $m_Z^2 = m_{Z,\mathrm{SM}}^2\big[1 + (\varepsilon^2 \tan^2\theta_w m_{Z,\mathrm{SM}}^2)/(m_{Z,\mathrm{SM}}^2 - m_k^2)\big]$. The coupling of K_μ^3 to the SM electromagnetic and neutral weak currents J_{em}^μ and J_Z is given by

$$\mathcal{L} \supset K_3^\mu \left(\varepsilon\, e J_{\mathrm{em}}^\mu - \varepsilon g \tan\theta_w \frac{m_k^2}{m_k^2 - m_Z^2} J_Z^\mu \right). \tag{11}$$

Note that eq. (7) implies a derivative coupling between K_3, ϕ, and the photon, as well as couplings of K_μ^1, K_μ^2 to the photon and the Z. The $K_1 K_2 \gamma$ coupling can be interpreted as a DM magnetic dipole moment. These operators lead to the annihilation processes $K_1K_1, K_2K_2 \to K_3\gamma$, $K_1K_2 \to \phi\gamma$, and $K_1K_1, K_2K_2 \to \gamma\gamma$, which are phenomenologically interesting as they feature mono-energetic photons (see also ref. [48]).

II.2. Relic Density

In the following, we investigate the DM relic density, in the $SU(2)_d$ model introduced in section II.1 as a function of the model parameters. To do so, we need to solve the Boltzmann equations describing $K_{1,2}$ annihilation and K_3 decay in the early Universe. The most relevant DM annihilation process is $K_1K_1, K_2K_2 \to K_3K_3$, the main properties of which are summarized in the first row of table I. Other annihilation channels, in particular $K_1K_1, K_2K_2 \to K_3\gamma$, $K_1K_2 \to \phi\gamma$, and $K_1K_2 \to f\bar{f}, W^+W^-$ (see table I) are all suppressed by ε^2. We do not consider $K_1K_1, K_2K_2 \to \gamma\gamma$ in the calculation because it is suppressed by a factor ε^4, but we still list it in table I. We will also disregard $K_1K_2 \to \phi\gamma$ in the following, assuming $m_\phi > 2m_k$. Finally, we neglect three-body annihilation processes like $K_1K_1 \to K_3K_3^* \to K_3\bar{f}f$. Their cross-sectionss are suppressed by ε^2 and by three-body phase space, and are therefore expected to be even smaller than those for annihilation to monoenergetic photon, $K_3\gamma$ and $\phi\gamma$.

The K_3 particles produced in $K_{1,2}$ annihilation decay to SM particles through their kinetic mixing. We will assume that this decay is faster than the Hubble rate at $T \lesssim m_k$, which is the case if

$$\varepsilon \gtrsim \sqrt{\frac{g_*^{1/2}}{\alpha_{\mathrm{em}}} \frac{m_k}{M_{\mathrm{Pl}}}} \tag{12}$$

where g_* is the total number of relativistic degrees of freedom in the Universe, α_{em} is the electromagnetic fine structure constant, and M_{Pl} is the Planck mass. If eq. (12) is fulfilled, the number density of K_3 follows its equilibrium value most of the time during DM freeze-out, but will deviate from equilibrium when n_{K_3} is very small and its decay is balanced by residual DM annihilation. If this is not the case, freeze-out can be significantly delayed and requires a significant increase in annihilation cross-section [16, 17]. $3 \to 2$ or $4 \to 2$ processes can also play an important role in reducing the DM abundance if the coupling g_d is large [16]. In this regime, where eq. (12) is violated, the temperature of the dark sector deviates significantly from that of the SM sector and evolves as $\sim \log a$, where a is the scale factor of the Universe. In our calculation, we focus on the parameter region where eq. (12) is fulfilled.

process	$v_{\rm rel}$-dependence	ε-dependence	freeze-out	CMB	Indirect Detection
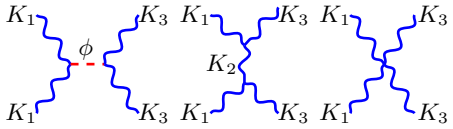	$\sqrt{\frac{v_{\rm rel}^2}{4}+\frac{2\Delta}{m_{\rm DM}}}$	1	dominant	negligible	✓
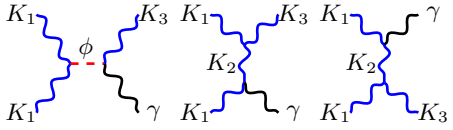	1	ε^2	subdominant	dominant	✓ (γ line)
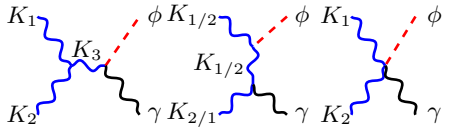	1	ε^2	subdominant (requires $m_\phi < 2m_k$)	dominant (requires $m_\phi < 2m_k$)	✓ (γ line if $m_\phi < 2m_k$)
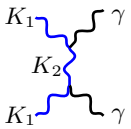	1	ε^4	negligible	negligible	negligible
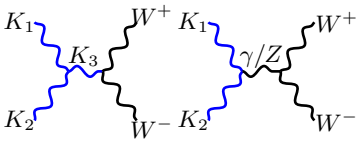	$v_{\rm rel}^2$	ε^2	subdominant	negligible	negligible
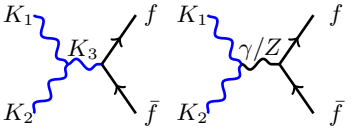	$v_{\rm rel}^2$	ε^2	subdominant	negligible	negligible

Table I. The dominant DM annihilation processes of the DM particles $K_{1,2}$ in the $SU(2)_d$ model. Note that the channel $K_1K_2 \to \phi\gamma$ is kinematically not accessible for $m_\phi \gtrsim 2m_k$. We list (from left to right), the Feynman diagrams contributing to a given process, its dependence on the relative velocity $v_{\rm rel}$ of the annihilating DM particles, its possible suppression by powers of the kinetic mixing parameter ε, and its relevance for DM freeze-out, CMB constraints, indirect and direct detection.

The decoupling of DM from the thermal bath is described by the following coupled Boltzmann equations:

$$\dot{n}_{12} + 3Hn_{12} = -\frac{1}{2}\langle\sigma v\rangle_{11\to 33}\left[n_{12}^2 - n_3^2\left(\frac{n_{12}^{\rm eq}}{n_3^{\rm eq}}\right)^2\right] - \frac{1}{2}\langle\sigma v\rangle_{11\to 3\gamma}\left[n_{12}^2 - (n_{12}^{\rm eq})^2\frac{n_3}{n_3^{\rm eq}}\right] - \frac{1}{2}\langle\sigma v\rangle_{12\to f\bar{f},W^+W^-}\left[n_{12}^2 - (n_{12}^{\rm eq})^2\right], \tag{13}$$

$$\dot{n}_3 + 3Hn_3 = \frac{1}{2}\langle\sigma v\rangle_{11\to 33}\left[n_{12}^2 - n_3^2\left(\frac{n_{12}^{\rm eq}}{n_3^{\rm eq}}\right)^2\right] + \frac{1}{4}\langle\sigma v\rangle_{11\to 3\gamma}\left[n_{12}^2 - (n_{12}^{\rm eq})^2\frac{n_3}{n_3^{\rm eq}}\right] - \Gamma_{K_3}\left[n_3 - n_3^{\rm eq}\right] \tag{14}$$

where n_{12} is the total number density of DM particles (K_1 and K_2 combined), n_3 is the number density of K_3, Γ_{K_3} is the K_3 decay rate, and the thermally averaged annihilation cross-sections $\langle\sigma v\rangle_{11\to 33}$, $\langle\sigma v\rangle_{11\to 3\gamma}$, and $\langle\sigma v\rangle_{12\to f\bar{f},W^+W^-}$ correspond to the processes $K_1K_1 \to K_3K_3$, $K_1K_1 \to$

$K_3\gamma$, and $K_1K_2 \to f\bar{f}, W^+W^-$, respectively. The annihilation cross-sections for $K_2K_2 \to K_3K_3$, and $K_2K_2 \to K_3\gamma$ are identical to the ones for $K_1K_1 \to K_3K_3$ and $K_1K_1 \to K_3\gamma$, respectively. Explicitly, we have

$$(\sigma v_{\rm rel})_{11\to 33} = \frac{g_d^4}{3072\pi m_k^2}\frac{2723 - 5472x_\phi + 2752x_\phi^2}{(1-x_\phi)^2}\sqrt{\frac{v_{\rm rel}^2}{4} + \frac{m_k^2 - m_{K_3}^2}{m_k^2}}\,, \tag{15}$$

$$(\sigma v_{\rm rel})_{11\to 3\gamma} = \frac{9g_d^4\varepsilon^2}{1024\pi m_k^2}\frac{31 - 68x_\phi + 38x_\phi^2}{(1-x_\phi)^2}\,, \tag{16}$$

$$(\sigma v_{\rm rel})_{12\to \phi\gamma} = \frac{g_d^4\varepsilon^2}{72\pi m_k^2}\,(1-x_\phi)\,(1+x_\phi)^2\,, \tag{17}$$

where we have introduced the notation $x_\phi \equiv m_\phi^2/(4m_k^2)$. The annihilation cross-sections for the processes $K_1K_2 \to f\bar{f}$ and $K_1K_2 \to W^+W^-$ are listed in appendix A. Note that we include only final state species lighter than m_k. The thermally averaged cross-sections $\langle\sigma v_{\rm rel}\rangle$ are obtained from these expressions along the lines of [49]. The decay rate Γ_{K_3} receives contributions from $K_3 \to f\bar{f}$ and from $K_3 \to W^+W^-$. The corresponding expressions are listed in appendix B.

The dark sector and SM sector are kept in equilibrium dominantly through $K_3 \to f\bar{f}$ decay and its inverse. Other 2-to-2 scattering or annihilation processes like $K_3 f \leftrightarrow \gamma f$, $K_3\gamma \leftrightarrow \bar{f}f$, $K_1K_2 \to \bar{f}f$ and $K_1 f \to K_2 f$ have a lower rate because the corresponding amplitudes are suppressed by an extra coupling constant. Moreover, scattering rates are typically proportional to $T \sim m_k/20$ at freeze-out, while decay rates are $\propto m_k$.

In fig. 2, we plot the solution to the Boltzmann equations, eqs. (13) and (14), for a specific set of model parameters as indicated in the plot. We see that DM freezes out at around $x_f \equiv m_k/T_f \sim 20$, similar to a conventional Weakly Interacting Massive Particle (WIMP). (This is only true because the K_3 decay rate is faster than the Hubble rate.) At late times, around $x \sim 50$, the number density n_3 of K_3 begins to deviate from its equilibrium value. At that time, n_3 is so small that K_3 production in residual DM annihilation comes into equilibrium with K_3 decay.

We study the parameter dependence of the DM relic density in fig. 3. The left panel in this figure shows the value of the $SU(2)_d$ gauge coupling g_d required to obtain the correct DM relic density as a function of the DM mass m_k and the kinetic mixing parameter ε (dashed black contours). We see that for large DM mass larger g_d is required to compensate for smaller annihilation cross-sections. At $10^{-6} \lesssim \varepsilon \lesssim 10^{-2}$, the relic density is independent of ε because the dominant annihilation process in this regime, $K_1K_1, K_2K_2 \to K_3K_3$ happens entirely in the dark sector. At $\varepsilon \gtrsim 10^{-2}$, the ε^2-suppressed annihilation channels to $K_3\gamma$, $f\bar{f}$, and W^+W^- also become significant, leading to distortion of the contours in fig. 3 (a). At very small ε, on the other hand, the K_3 decay rate drops below the Hubble rate. The lingering K_3 can annihilate back to $K_{1,2}K_{1,2}$, thus reducing the net DM annihilation rate and delaying freeze-out unless g_d is increased or m_k is lowered. In this regime, "cannibal processes" such as $K_1K_1K_2 \to K_1K_3$ need to be taken into account [16]. We also note the small dip in the $g_d = \text{const}$ contours in fig. 3 (a) around $m_k = m_Z$. In this region, the mixing between K_3 and the Z is large even for very small ε.

II.3. Direct Detection

Direct detection of Impeded DM in the $SU(2)_d$ model is complementary to indirect searches as it is sensitive to the $K_1K_2f\bar{f}$ coupling, which does not contribute significantly to DM annihilation, being velocity and ε^2 suppressed (see table I). The relevant processes for direct detection are the spin-independent t-channel reactions $K_{1,2}q \to K_{2,1}q$, mediated by γ, Z, and K^3. Since the typical

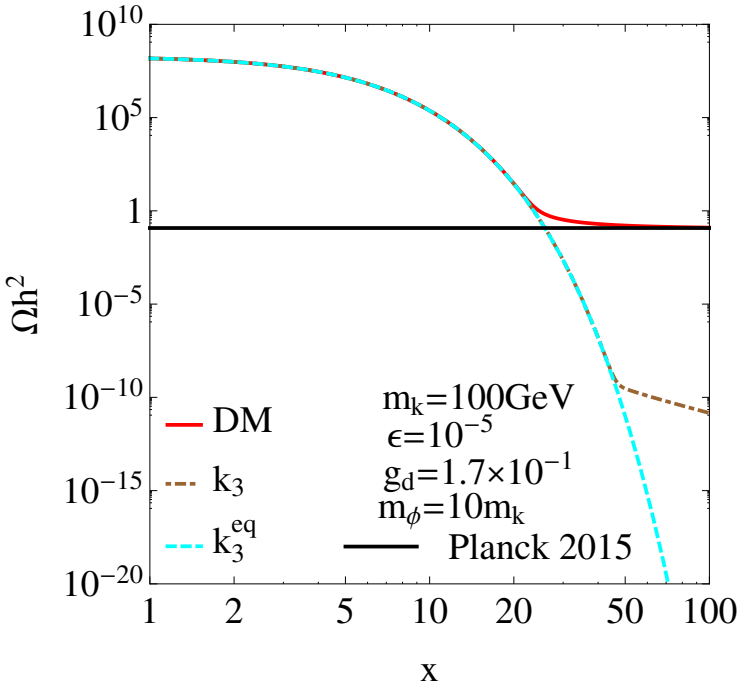

Figure 2. The evolution of the effective present day energy density Ωh^2 of DM particles $K_{1,2}$ and of the DM annihilation product K_3 for a particular choice of parameters in the $SU(2)_d$ model. Ωh^2 is obtained by scaling the instantaneous number density by the subsequent expansion of the Universe and normalizing to the critical density today. We see that the density of K_1, K_2 (red) begins to deviate from its equilibrium value (turquoise) around $x \equiv m_k/T \sim 20$, while K_3 (brown) stays in equilibrium until $x \sim 50$. Note that for much smaller kinetic mixing ε, the K_3 decay rate can become lower than the Hubble rate, substantially delaying DM freeze-out. (This situation was dubbed "co-decaying DM" in ref. [16]).

momentum transferred in DM–nucleus scattering is $\ll m_k, m_Z$, the photon mediated diagram dominates over the Z and K_3 mediated diagrams, so we neglect the latter. In principle, the dark Higgs boson ϕ can also mediate DM–nucleus scattering via mixing with the SM Higgs through the Higgs portal, eq. (5). However, the corresponding amplitudes are suppressed by the mass of ϕ, the small Yukawa couplings of the Higgs, and by our assumption that Higgs mixing is tiny. Therefore, we neglect ϕ-mediated scattering here.

The spin-independent (SI) DM–nucleus scattering cross-section in the $SU(2)_d$ model is

$$\frac{d\sigma_{\rm SI}}{dE_r} = \frac{2\pi\alpha_{\rm em}\alpha_d(Z\varepsilon)^2}{3m_k^2 E_r}\left(1+\frac{E_r}{4E_{\rm in}}\frac{m_N^2-2m_k m_N-m_k^2}{m_k m_N}\right)F_{\rm SI}^2(E_r)\,, \tag{18}$$

where E_r is the nuclear recoil energy, Z is the nuclear charge, $\alpha_{\rm em} \equiv e^2/(4\pi)$ and $\alpha_d \equiv g_d^2/(4\pi)$ are the electromagnetic and $SU(2)_d$ fine structure constants, respectively, $E_{\rm in} = m_k v_{\rm in}^2/2$ is the kinetic energy of the incoming DM particle, and $F_{\rm SI}(E_r)$ is the nuclear form factor [94]. To obtain the spin-independent result in eq. (18), we have computed the scattering of K_1, K_2 on a scalar particle of charge Z, thus neglecting the nuclear spin. Spin-dependent scattering exists as well, but as usual constraints are much weaker as the Z^2 enhancement is absent. Note that eq. (18) has some similarity with the scattering cross section for dipolar dark matter [95, 96]. This is not surprising as we argued in section II.1 that the $K_1K_2\gamma$ coupling is in fact a magnetic dipole coupling.

To calculate direct detection constraints, we use data from the LUX experiment corresponding to 332 live days [97], (see also PandaX-II results [52] from first 98.7-day data, which has comparable

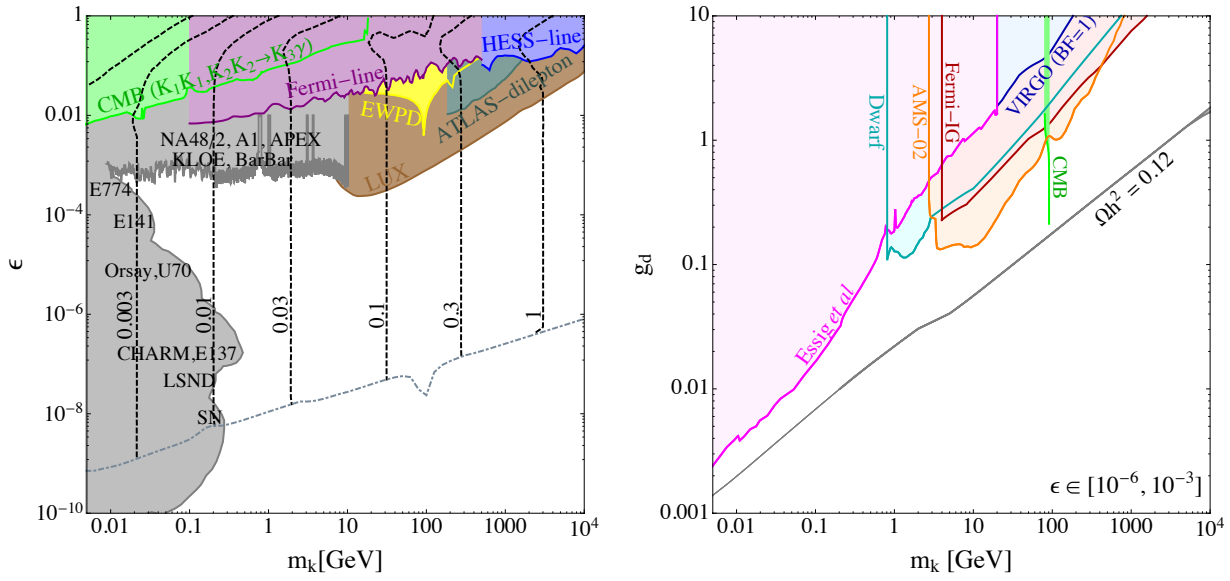

(a) (b)

Figure 3. (a): Parameter space for the dark $SU(2)_d$ model of Impeded DM as a function of DM mass m_k and kinetic mixing parameter ε. Dashed black lines indicate, for each combination of m_k and ε, the value of the dark sector gauge coupling g_d required to obtain the correct DM relic density. Shaded regions show constraints from direct detection (LUX, brown) [50, 51] (see also PandaX-II [52]), the CMB (light green) [53], gamma ray line searches in Fermi-LAT (purple) [54] and H.E.S.S. (blue) [55], collider searches (ATLAS dilepton, dark green) [56], electroweak precision data (EWPD, yellow) [57], and dark photon searches (gray) [58–88]. In the region below the dot-dashed gray line, $\Gamma_{K_3} < \mathrm{H}(T = m_k)$ and the model is in the "co-decaying" regime [16]. Constraints labeled with "-line" correspond to bounds on a monoenergetic gamma ray flux from $K_1K_1, K_2K_2 \to K_3\gamma$. (b): Constraints in the m_k vs. g_d plane in the region $10^{-6} \lesssim \varepsilon \lesssim 10^{-3}$, in which the DM relic density is independent of ε. In the gray band, the correct density is obtained. We compare to constraints from Fermi-LAT gamma ray searches in dwarf galaxies (cyan) [89, 90], in the Virgo cluster (dark blue) [91], and in the inner Milky Way (dark red) [92], to exclusion limits from AMS-02 positron data (orange), and to a combination of x-ray and gamma-ray bounds from a compilation by Essig et al. (magenta) [93]. We plot the CMB constraint for a narrow window $m_k \in [m_{W,\mathrm{SM}}, m_{Z,\mathrm{SM}}]$ where $\Delta > 0$ and use $\varepsilon = 10^{-3}$ for this constraint.

limit to LUX). The LUX constraint is presented in ref. [97] as a mass-dependent limit on the total DM–nucleon scattering cross-section σ_n, assuming the latter to be independent of the DM velocity. This assumption is violated for the photon-mediated scattering processes relevant in our $SU(2)_d$ model. Therefore, we first compute σ_n in a contact operator model with a fermionic DM candidate χ, for instance $\mathcal{L} \supset \bar{\chi}\gamma_\mu\chi\bar{q}\gamma^\mu q$ and choose the coupling such that the LUX limit is saturated. We then compute the differential event rate dR/dE_r for this operator, taking into account the Maxwell–Boltzmann-like DM velocity distribution, and multiply by the efficiency for nuclear recoil events in LUX [51]. We integrate dR/dE_r over the energy range $1.1\,\mathrm{keV} < E_r < 100\,\mathrm{keV}$ to obtain the maximum total number of events $N^{\max}$ consistent with LUX data. We then compute $\int dE_r\, dR/dE_r$ also in our model. By requiring the result to match $N^{\max}$ determined for the contact operator, we obtain a constraint on the coupling g_d. This constraint is shown in fig. 3 (a) in brown. We see that it is stronger than indirect bounds and collider bounds for DM masses between 10 GeV and 10 TeV.

II.4. Constraints from the Cosmic Microwave Background

Another important constraint on any model in which DM can annihilate arises from observations of the cosmic microwave background (CMB). In particular, the extra energy injected into the primordial plasma due to DM annihilation would delay recombination and thus leave observable imprints in the CMB [98–101]. The impact of DM on the CMB is characterized by the "energy deposition yield" [102, 103]

$$p_{\rm ann} = f_{\rm eff}\frac{\langle\sigma v\rangle}{m_{\rm DM}}\,. \tag{19}$$

Here, $f_{\rm eff}$ gives the efficiency with which the energy released in DM annihilation is absorbed by the primordial plasma.

For the specific case of the $SU(2)_d$ model, we need to consider the annihilation processes shown in table I. As in the previous sections, we neglect DM annihilation to $\phi\gamma$, assuming that ϕ is sufficiently heavy for this channel to be closed. We also note that annihilation via $K_1K_2 \to f\bar{f}, W^+W^-$ is subdominant at the CMB epoch because of $v_{\rm rel}^2$ and ε^2 suppression, as is $K_1K_1, K_2K_2 \to \gamma\gamma$ because of ε^4 suppression.

The annihilation cross-section for $K_1K_1, K_2K_2 \to K_3K_3$ is phase space suppressed by the factor $\sqrt{v_{\rm rel}^2/4 - 2\Delta/m_k}$, therefore we need to estimate the DM velocity at the time of CMB decoupling. To do so, we need to determine the temperature at which DM kinetically decouples from the SM, i.e. the temperature at which $K_{1,2}f \to K_{2,1}f$ scattering freezes out. (Scattering of $K_{1,2}$ on photons via t-channel $K_{1,2}$ exchange is negligible as the cross-section is proportional to ε^4.) It turns out that, in most of the parameter space considered here, this happens no later than at $T \gtrsim 1\,\text{MeV}$, when e^+e^- annihilation reduces the density of SM fermions by ~ 10 orders of magnitude. Afterwards, the kinetic energy of DM drops quickly as a^{-2}, where a is the scale factor of the Universe. Therefore, by the time of recombination, the dark sector temperature has dropped to $\lesssim 10^{-6}\,\text{eV}$. We conclude that, at the CMB epoch the DM temperature is typically too low to overcome the mass splitting $|\Delta| \sim m_k\varepsilon^2$ in the process $K_1K_1, K_2K_2 \to K_3K_3$, except at very small ε and in a small mass window with $m_{W,\rm SM} < m_k < m_{Z,\rm SM}$ where $\Delta > 0$ (see eq. (10)). We plot the CMB constraint from $K_1K_1, K_2K_2 \to K_3K_3$ in this narrow window, for $\varepsilon = 10^{-3}$ in fig. 3 (b). We see that the resulting limit is $g_d \lesssim 0.2(10^{-3}/\varepsilon)^{1/4}$.

Finally, we need to consider the annihilation process $K_1K_1, K_2K_2 \to K_3\gamma$. For this annihilation channel, $f_{\rm eff}$ can be written as

$$f_{\rm eff} = \frac{E_{K_3}}{E_{K_3}+E_\gamma} f_{\rm eff}^{K_3}(E_{K_3}) + \frac{E_\gamma}{E_{K_3}+E_\gamma} f_{\rm eff}^{\gamma}(E_\gamma)\,, \tag{20}$$

where $E_{K_3} \approx \frac{5}{4}m_k$ and $E_\gamma \approx \frac{3}{4}m_k$. In eq. (20), the contributions to $f_{\rm eff}$ from K_3 ($f_{\rm eff}^{K_3}$) and from photons ($f_{\rm eff}^{\gamma}$) is weighted by respective energy fraction because the CMB is sensitive to energy injection into the primordial plasma. $f_{\rm eff}^{K_3}$ is given by

$$f_{\rm eff}^{K_3}(E_{K_3}, m_k, \varepsilon) \approx \sum_i \text{BR}_{K_3\to SM_iSM_i}(m_k,\varepsilon) f_{\rm eff}^{SM_iSM_i}(E_{K_3}/2)\,. \tag{21}$$

Here, the sum runs over all SM final states into which K_3 can decay, and $f_{\rm eff}^{SM_iSM_i}$ are the corresponding efficiency factors for each final state. We take these, as well as $f_{\rm eff}^{\gamma}$ from ref. [104]. We make the approximation here that the energy of each SM_i particle is $E_{K_3}/2$ in the laboratory frame. Their actual energy is distributed around $E_{K_3}/2$, but since the energy of K_3 is very close to its mass m_k, the distribution is very close to a delta function. Moreover, $f_{\rm eff}^{SM_iSM_i}$ changes only mildly with

E_{SM_i}, therefore our assumption is reasonable. For m_k smaller than the QCD scale, the calculation of $f_{\rm eff}^{K_3}$ follows the procedure from ref. [105]. Demanding $p_{\rm ann} < 4.1 \times 10^{-28}\,{\rm cm}^3\ {\rm s}^{-1}\ {\rm GeV}^{-1}$ [53], we obtain the constraints shown in green in fig. 3 (a). We see that CMB constraints from $K_1K_1, K_2K_2 \to K_3\gamma$ are particularly strong at low DM mass, where the annihilation cross-section is large. In conventional WIMP models, they exclude thermal relic DM lighter than ~ 10 GeV, while in our $SU(2)_d$ model, they can always be avoided by choosing $\varepsilon \lesssim 10^{-2}$, a condition that is imposed anyway by dark photon searches (gray region in fig. 3 (a)).

II.5. Indirect Detection

In this section, we will investigate indirect astrophysical constraints on Impeded DM in the $SU(2)_d$ model, in particular from searches for anomalous signals in continuum gamma rays, charged cosmic rays, and gamma ray lines.

The differential flux of continuum photons from a solid angle interval $d\Omega$ is

$$\frac{d\Phi}{dE_\gamma d\Omega} = \frac{1}{8\pi\, c\, m_{\rm DM}^2} J(\theta,\phi) \sum_X \langle\sigma v\rangle_X \frac{dN_\gamma^X}{dE_\gamma}\,, \tag{22}$$

where $\langle\sigma v\rangle_X$ is the thermally averaged annihilation cross-section for a process X, dN_γ^X/dE_γ is the differential photon spectrum for a single annihilation reaction, and the sum runs over all accessible final states. The factor c is a symmetry factor, which is $c = 4$ for vector DM. It would be $c = 1$ ($c = 2$) if DM was a Majorana (Dirac) fermion.[3] The factor $J(\theta,\phi)$ in eq. (22) is the integral over the squared DM density along the line of sight (l.o.s.) oriented in direction (θ,ϕ). It is given by

$$J(\theta,\phi) = \int_{\rm l.o.s.} ds\, \rho_{\rm DM}^2(s,\theta,\phi)\,. \tag{23}$$

We describe $\rho_{\rm DM}$ as an NFW profile with a local DM density $\sim 0.3\,{\rm GeV/cm}^3$ [106–108], and a scale radius of 20 kpc. The cosmic ray e^+ and e^- spectra are obtained from an expression analogous to eq. (22), replacing dN_γ^X/dE_γ by the corresponding spectra $dN_{e^\pm}^X/dE_{e^\pm}$.

The dominant contribution to continuum gamma ray and charged cosmic ray signals in the $SU(2)_d$ model comes from the annihilation channel $K_1K_1, K_2K_2 \to K_3K_3$. Even though we have seen above that this process is kinematically forbidden at the CMB epoch, it opens up again later, when DM particles are reaccelerated as they fall into the gravitational potential wells of newly forming galaxies and clusters. Observable signals arise from $K_1K_1, K_2K_2 \to K_3K_3$ when K_3 decays to SM particles through its kinetic mixing with the photon and the Z. These decays contribute to cosmic e^+ and e^- fluxes through $K_3 \to e^+e^-$, and to e^+, e^-, and to gamma ray fluxes through final state radiation and $K_3 \to$ mesons, followed by meson decays. For $m_k \lesssim 3\,{\rm GeV}$, we compute the spectra $dN_{e^\pm,\gamma}/dE_{e^\pm,\gamma}$ from $e^+e^- \to$ hadrons data following ref. [105]. At larger m_k, we compute the K_3 decay rates to quark and lepton pairs and then use ref. [109] to obtain the resulting cosmic ray spectra.

The high-energy e^+ and e^- can also upscatter ambient photons to gamma-ray energies via inverse Compton scattering (ICS), providing an additional secondary contribution to the gamma-ray flux. This contribution depends on the propagation of the charged particles, and so has additional uncertainties relative to the prompt photon emission from annihilation. For the constraints we discuss below, only those from Fermi observations of the Virgo cluster include the ICS component.

[3] While the symmetry factor is different for different types of DM, the thermal relic cross-sections for different candidates are modified by an identical factor, so that the expected gamma ray flux is independent of c.

We also consider DM annihilation to final states containing mono-energetic photons, where the dominant signal channel is $K_1K_1, K_2K_2 \to K_3\gamma$. In this case dN_γ^X/dE_γ is just a δ function. As in the previous sections, we do not consider $K_1K_2 \to \phi\gamma$, assuming this channel to be kinematically forbidden.

We compare the predicted cosmic ray spectra to the following data sets

- **Fermi-LAT observations of dwarf galaxies.** We use the bin-by-bin likelihood provided by the Fermi-LAT collaboration [89], based on observations of 15 non-overlapping dwarf galaxies. Using eq. (15), we can translate this likelihood into limits on the annihilation cross-section $\langle\sigma v_{\rm rel}\rangle_{11\to33}$ and hence g_d. In computing $\langle\sigma v_{\rm rel}\rangle_{11\to33}$, we account for the different root mean square (rms) velocity v_0 in each dwarf galaxy, and we use $\langle v_{\rm rel}\rangle = (2/\sqrt{\pi})v_0$. This approach is valid in the regime where the cross-section is linearly dependent on velocity; in the forbidden regime where $\varepsilon > v_0$, it may mis-estimate $\langle\sigma v_{\rm rel}\rangle$ (since in this case the cross-section will be sensitive to the high-velocity tail of the velocity distribution), but in this regime the cross-section will in any case be very small.

- **Fermi-LAT observations of the Virgo cluster.** This constraint is based on three years of Fermi-LAT data, presented in ref. [91] as upper limits on $\langle\sigma v_{\rm rel}\rangle_{{\rm SM}_i{\rm SM}_i}(m_{\rm DM})$, the thermally averaged DM annihilation cross-section into different final states consisting of pairs of SM particles ${\rm SM}_i$. We impose that

$$\frac{2}{c}\Big[\langle\sigma v_{\rm rel}\rangle_{11\to33} + \langle\sigma v_{\rm rel}\rangle_{22\to33}\Big]\Big[({\rm BR}_{K_3\to{\rm SM}_i{\rm SM}_i})^2 + {\rm BR}_{K_3\to{\rm SM}_i{\rm SM}_i}\big(1-{\rm BR}_{K_3\to{\rm SM}_i{\rm SM}_i}\big)\Big] \tag{24}$$

  should be below the limiting value of $\langle\sigma v_{\rm rel}\rangle_{{\rm SM}_i{\rm SM}_i}(m_k/2)$. Here, c is the same symmetry factor as in eq. (22), and the last term describes the average number of K_3 decays to ${\rm SM}_i{\rm SM}_i$. In computing $\langle\sigma v_{\rm rel}\rangle_{11\to33}$ and $\langle\sigma v_{\rm rel}\rangle_{22\to33}$, we use the rms velocity of the Virgo cluster, $v_0 = 525\,{\rm km/sec}$, and set again $\langle v_{\rm rel}\rangle = (2/\sqrt{\pi})v_0$. We find that the most constraining K_3 decay modes are $\tau^+\tau^-$ at $m_k \lesssim 40{\rm GeV}$, $b\bar{b}$ at intermediate $m_k \in [40, 200]\,{\rm GeV}$, and e^+e^- at $m_k \gtrsim 200{\rm GeV}$. The strong constraint on annihilation to e^+e^- at high masses arises from inverse Compton scattering of the electrons on the CMB, which produces photons in the Fermi-LAT energy range. Note that the authors of [91] multiply the DM annihilation cross-section by a boost factor to account for enhanced annihilation in overdense DM subhalos. We do not include boost factors here because (a) the size of this boost factor is highly uncertain, so constraints assuming a large boost factor are difficult to make robust, and (b) since the rms velocity in DM subhalos is much lower than in the host halo, $\langle\sigma v_{\rm rel}\rangle_{11\to33}$ and $\langle\sigma v_{\rm rel}\rangle_{22\to33}$ will be lower for DM particles bound in subhalos, especially for the very small subhalos that typically contribute much of the boost.

- **Gamma ray constraints from the inner Milky Way.** These limits are derived in analogy to the Virgo limits, but based on the results of ref. [92], assuming an NFW profile for the Milky Way. We assume an rms velocity $v_0 = 220\,{\rm km/sec}$ for the Milky Way, but we remind the reader that the velocity dispersion in the Galactic Center region is highly uncertain, see for instance [110].

- **Combined x-ray, gamma ray, and e^+e^- limits for light DM.** For low mass DM ($1\,{\rm MeV} \lesssim m_k \lesssim 10\,{\rm GeV}$), Essig *et al.* [93] have compiled x-ray and gamma ray constraints for the annihilation channel ${\rm DM\,DM} \to e^+e^-$. They use data from the HEAO-1 [111], INTEGRAL [112], COMPTEL [113], EGRET [114], and Fermi [115] satellites. We translate

these limits into bounds on g_d in the same way as for Fermi-LAT limits from the Virgo cluster and the Milky Way.

- **AMS-02 data on e^+ and e^- fluxes.** Monoenergetic e^+e^- pairs produced in K_3 decays can generate bump-like features in the cosmic electron and positron fluxes observed by AMS-02. We use in particular the AMS-02 measurement of the positron flux [116] and follow the approach of ref. [90] to derive a bound on $\langle\sigma v_{\rm rel}\rangle_{33}$ from it. In computing $\langle\sigma v_{\rm rel}\rangle_{33}$, we assume $v_0 = 220\,\text{km/sec}$. Note that our bound is more conservative than the one from ref. [117] since we assume larger magnetic fields in simulating e^+e^- propagation [118, 119].

- **Gamma ray line searches in Fermi-LAT and H.E.S.S.** Even though the cross-section for $K_1K_1, K_2K_2 \to K_3\gamma$ is suppressed by ε^2, we expect competitive limits from these channels thanks to the cleanliness of gamma ray line signatures. We derive these limits using the data from ref. [54, 55] [4], (see also [121]).

The above results are summarized in fig. 3 (b). We see that AMS-02 provides the most stringent constraints for $3\,\text{GeV} \lesssim m_k \lesssim 400\,\text{GeV}$, followed by gamma ray constraints from the inner galaxy. The constraints from Fermi-LAT gamma ray searches in dwarf galaxies provide the strongest bound for DM masses around a few GeV, where the annihilation products mostly lie below the energy threshold of AMS-02. The dwarf bounds are only a factor of few weaker than those from AMS-02 and Fermi observations of the inner Galaxy over the remainder of the mass range, and have smaller systematic uncertainties. At DM masses below 1 GeV, the dominant decay channel of K_3 is e^+e^-. In this case, the strongest constraint arises from limits on x-ray and gamma ray photons produced as final state radiation from DM annihilation in the Milky Way. Galactic observations offer on the one hand large statistics, and on the other hand large DM velocities, which is important for the $v_{\rm rel}$-suppressed annihilation channel $K_1K_1, K_2K_2 \to K_3K_3$. Note that when $\varepsilon \gtrsim 10^{-3}$ (above the range assumed in fig. 3 (b), and in tension with other limits according to fig. 3 (a)), $|\Delta|$ is large and shuts off the $K_1K_1, K_2K_2 \to K_3K_3$ channel, see eq. (15). This happens first in dwarf galaxies, where v_0 is lowest.

III. DARK PIONS AS IMPEDED DM WITH $\Delta > 0$

III.1. Model

We now switch gears and discuss a second realization of Impeded DM in a concrete model. In particular, we introduce a composite hidden sector based on an $SU(N) \times U(1)'$ gauge symmetry, analogous to the strong and electromagnetic interactions of the SM (see refs. [3, 4, 6, 122–135] for similar models). We assume the existence of two species of light "dark quarks" u_d and d_d with the charge assignments listed in table II. We also introduce a dark scalar field ϕ that breaks $U(1)'$ by two units, giving mass to the dark photon. In analogy to QCD, the global chiral symmetry of the dark quarks is broken at energies below the strong coupling scale Λ_N. The associated Nambu–Goldstone bosons (dark pions), π_d^+, π_d^- constitute excellent DM candidates, stabilized by a Z_2 symmetry, a residual of the broken dark $U(1)'$ symmetry. (Note that the superscripts here refer to the $U(1)'$ charge of the dark pions, not an electromagnetic charge.) Their neutral partner, π_d^0, is unstable and can decay through the chiral anomaly to dark photons.

In the broken phase of chiral symmetry, the effective Lagrangian of the model is [126]

$$\mathcal{L} = \frac{1}{4} f_\pi^2 \,\text{Tr}\left[\partial_\mu U^\dagger \partial^\mu U\right] + \mu \frac{f_\pi^2}{2} \,\text{Tr}\left[U^\dagger M + M^\dagger U\right], \tag{25}$$

[4] Ref. [55] has translated the H.E.S.S. limits [120] from Einasto profile to NFW profile.

	SU(N)	$U(1)'$
u_d	$\square$	$2/3$
d_d	$\square$	$-1/3$
ϕ	1	2

Table II. Field content and quantum numbers of the dark pion model, where $\square$ stands for the fundamental representation of the dark $SU(N)$. We show here only the field content necessary for the Impeded DM phenomenology, but it is important to keep in mind that additional particles like heavy dark leptons are necessary for anomaly cancellation.

where we will refer to f_π as the dark pion decay constant (even though the dark $\pi_d^\pm$ are stable). The matrix U is defined as $U \equiv \exp(i\pi_d^a \sigma^a / f_\pi)$ with the Pauli matrices σ^a, M is the 2×2 mass matrix for u_d and d_d, and

$$\pi_d^a \sigma^a = \begin{pmatrix} \pi_d^0 & \sqrt{2}\pi_d^+ \\ \sqrt{2}\pi_d^- & -\pi_d^0 \end{pmatrix} . \tag{26}$$

Note that the mass matrix M is diagonal; since ϕ carries two units of $U(1)'$ charge, it cannot induce mixing between u_d and d_d even after breaking $U(1)'$.

Dark pion DM can behave as Impeded DM if there is a mass splitting between $\pi_d^\pm$ and π_d^0. Such a mass splitting could have two different origins: different u_d and d_d masses, $m_{u_d} \neq m_{d_d}$, and $U(1)'$ radiative corrections. We assume for simplicity that u_d and d_d are degenerate in mass, i.e. that dark isospin is unbroken. This means in particular that we neglect the η_d^0 meson, which could mix with π_d^0 if $m_{u_d} \neq m_{d_d}$. Such mixing would be proportional to $m_{u_d} - m_{d_d}$ and would give a mass splitting between $\pi_d^\pm$ and π_d^0 of order $(m_{u_d} - m_{d_d})^2 m_{\pi_d^\pm}^3 / [2(m_{u_d} + m_{d_d})^2 m_{\eta_d^0}^2]$ [126].

The mass splitting between $\pi_d^\pm$ and π_d^0 is then obtained from the self-energy diagrams of $\pi_d^\pm$ through A'. For light A', the mass splitting is estimated to be [136–139],

$$m_{\pi_d^\pm}^2 - m_{\pi_d^0}^2 \approx \frac{g'^2}{16\pi^2} \Lambda_N^2 \tag{27}$$

$$\Delta \equiv m_{\pi_d^\pm} - m_{\pi_d^0} \approx \frac{g'^2}{16\pi^2} \frac{\Lambda_N^2}{2m_\pi} . \tag{28}$$

In the following, we use the value $\Lambda_N = 4\pi f_\pi$ for the dark sector confinement scale. Note that Δ in the dark pion model is always positive, i.e. DM is always heavier than its annihilation product π^0. Thus, annihilation is never kinematically forbidden.

In the following, we will also need the rate of the anomaly-mediated decay $\pi_d^0 \to A'A'$, which we calculate to be

$$\Gamma(\pi_d^0 \to A'A') = \frac{g'^4 m_\pi^3}{1024\pi^5 f_\pi^2} \left(1 - \frac{4m_A'^2}{m_\pi^2}\right)^{3/2} . \tag{29}$$

III.2. Constraints from relic abundance, direct and indirect detection

Annihilation of the DM particles $\pi_d^\pm$ in the dark pion scenario is dominated by the process $\pi_d^+\pi_d^- \to \pi_d^0\pi_d^0$. The amplitude for this reaction is $\mathcal{M}(\pi_d^+\pi_d^- \to \pi_d^0\pi_d^0) = (s - m_\pi^2)/f_\pi^2$ [140], where $m_\pi \equiv m_{\pi_d^\pm}$ is the dark pion mass. The cross-section is then given by

$$\begin{aligned}(\sigma v_{\rm rel})_{00} &= \sigma_0 \times \sqrt{\frac{v_{\rm rel}^2}{4} + \frac{2\Delta}{m_\pi}} \\ &\simeq 6\times 10^{-26}{\rm cm}^3\,{\rm sec}^{-1} \times \left(\frac{m_\pi/f_\pi^2}{7\times 10^{-4}{\rm GeV}^{-1}}\right)^2 \quad \text{at freeze-out,}\end{aligned} \tag{30}$$

where $\sigma_0 = 9/(64\pi)m_\pi^2/f_\pi^4$. The estimate in the second line of eq. (30) is for the time of DM freeze-out, where $v_{\rm rel} \sim 0.47$, and assuming $\Delta/m_\pi \ll 1$. From the requirement of obtaining the correct thermal relic cross-section, we then obtain

$$\frac{m_\pi}{f_\pi^2} \sim 7\times 10^{-4}\,{\rm GeV}^{-1}\,. \tag{31}$$

In the following, we will use this condition to determine f_π as a function of m_π.

DM can annihilate also via $\pi_d^+\pi_d^- \to A'A'$, with cross-section

$$(\sigma v_{\rm rel})_{A'A'} \simeq \frac{g'^4}{8\pi m_\pi^2}\left(1 - \frac{m_{A'}^2}{m_\pi^2} + \frac{3m_{A'}^4}{8m_\pi^4}\right)\frac{\sqrt{1-m_{A'}^2/m_\pi^2}}{\left[1-m_{A'}^2/(2m_\pi^2)\right]^2}\,. \tag{32}$$

In the following, we will neglect this second annihilation channel on the grounds that the $U(1)'$ gauge coupling g' should be much smaller than the m_π/f_π to keep the model QCD-like. Requiring that $(\sigma v_{\rm rel})_{A'A'} < 0.1(\sigma v_{\rm rel})_{00}$ leads to the requirement $g' \lesssim 0.01\sqrt{m_\pi/{\rm GeV}}$. In fig. 4, where we plot the parameter space of the dark pion model, this condition is satisfied below the diagonal black line.

To keep π_d^0 in thermal equilibrium with the SM sector throughout DM freeze-out, the dark sector should have appreciable interactions with SM particles. This can be achieved for instance through a kinetic mixing term of the A',

$$\mathcal{L} \supset \frac{\varepsilon}{2}F'_{\mu\nu}F^{\mu\nu}\,, \tag{33}$$

where $F_{\mu\nu}$ and $F'_{\mu\nu}$ are the field strength tensors of the photon and the A', respectively. Requiring the scattering rate for $A' + f \to \gamma + f$ to be larger than the Hubble rate at freeze-out gives the constraint

$$\varepsilon \gtrsim \mathcal{O}(10^{-8})\sqrt{m_\pi/{\rm GeV}}\,. \tag{34}$$

Note that A' decay to $f\bar{f}$ and its inverse are less efficient than $A' + f \to \gamma + f$ in keeping A' in thermal equilibrium at $\pi^\pm$ freeze out if $m_{A'} \ll m_\pi$. If the A' mass is similar to m_π, then A' decay and scattering will have similar efficiency in keeping A' in equilibrium. Demanding also that π_d^0 and A' are in equilibrium through $\pi_d^0 \leftrightarrow A'A'$ leads to the additional requirement

$$g' \gtrsim \mathcal{O}(10^{-3})(f_\pi^2 m_\pi^{-1}{\rm GeV}^{-1})^{1/4} \sim 5\times 10^{-3}\,. \tag{35}$$

This condition is satisfied above the horizontal gray line in fig. 4.

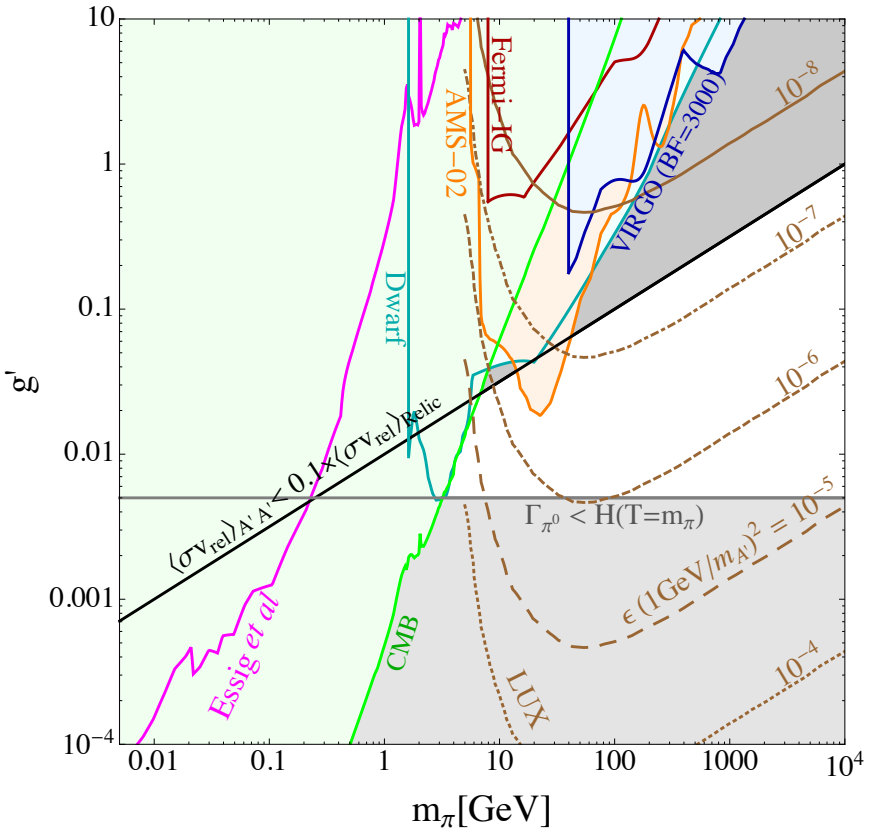

Figure 4. Constraints on the parameter space of the dark pion model from direct detection data [50, 51] and indirect searches. The indirect detection constraints are similar to those shown in fig. 3 (b). We focus on the annihilation process $\pi_d^+\pi_d^- \to \pi_d^0\pi_d^0$. For each combination of m_π and g', the dark pion decay constant f_π is determined from the relic density requirement eq. (31). In the large-g' region above the diagonal black line, this condition is not strictly valid as annihilation via $\pi_d^+\pi_d^- \to A'A'$ becomes relevant. In the region below the horizontal gray line, the relic density is modified by a small π_d^0 width, preventing π_d^0 from maintaining equilibrium with the SM.

In direct detection experiments, dark pion DM can scatter on protons via t-channel A' exchange. The scattering cross-section is

$$\sigma_p = \varepsilon^2 e^2 g'^2 \frac{(m_\pi m_p)^2}{\pi m_{A'}^4 (m_\pi + m_p)^2} \simeq 10^{-47}\,\text{cm}^2 \left(\frac{g'}{10^{-2}}\right)^2 \left(\frac{\varepsilon}{10^{-7}}\right)^2 \left(\frac{1\,\text{GeV}}{m_{A'}}\right)^4 . \tag{36}$$

Based on this expression, we derive constraints on the model parameters from LUX data [50, 51]. The result is shown in fig. 4 (brown contours) for different values of $\varepsilon(1\,\text{GeV}/m_{A'})$, as indicated in the plot.

Dark pion DM is also constrained by indirect astrophysical observations, where annihilation via $\pi_d^+\pi_d^- \to \pi_d^0\pi_d^0$, followed by $\pi_d^0 \to A'A'$ and $A' \to \text{SM}\,\overline{\text{SM}}$ leaves an imprint. We show the resulting constraints in fig. 4. In this plot, we have taken $m_{A'} \sim m_{\pi_d^0}/2$, so that A' particles decay nearly at rest. Changing the mass of A' will not dramatically change our result. Constraints are obtained in the same way as for the $SU(2)_d$ model, see sections II.4 and II.5.

As in the $SU(2)_d$ model, the DM velocity relevant for CMB bounds is much smaller than $\sqrt{\Delta/m_\pi}$, so that eq. (30) reduces to

$$(\sigma v_{\rm rel})_{00} \simeq 10^{-23}{\rm cm}^3{\rm s}^{-1}\frac{g'}{m_\pi/{\rm GeV}}\,, \tag{37}$$

where we have again determined f_π from eq. (31), and Δ from eq. (28).

In fact, for the dark pion model, $v_{\rm rel}^2 < \Delta/m_\pi$ holds even in galaxy clusters as long as g' is not tiny. It holds in particular for g' large enough to keep π_d^0 in equilibrium in the early Universe, i.e. above the horizontal gray line in fig. 4. Therefore, we can always compute the annihilation cross-section using the $v_{\rm rel}$-independent expression in eq. (37). However, we now include substructure enhancement in the computation of limits from the Virgo cluster. In the plot we have used a substructure boost factor of 3 000 for the Virgo cluster. Such large boost factors may exist if there is sufficient small-scale substructure (as discussed in [91]), although assuming them could lead to overly stringent constraints. We see, however, that even for such large boost factors, the limits from Virgo are superseded by other bounds.

We see from fig. 4 that constraints from dwarf galaxies and from AMS-02 are strongest for m_π above few GeV, just as they were for the $SU(2)_d$ model in fig. 3. The constraints on the e^+e^- final state by Essig et al. [93] also provide interesting limits on the dark pion model, but they are weaker than bounds from the CMB, which give the strongest constraints at $m_\pi \lesssim$ GeV. The reason why CMB bounds are so powerful in the dark pion model, while being subdominant in the $SU(2)_d$ model from section II is of course the different sign of Δ: for $\Delta > 0$, as in the dark pion model, DM annihilation can be significant even at very small DM velocity.

Figure 4 shows that the dark pion model is not constrained by indirect searches for $m_\pi \gtrsim \mathcal{O}(1)$GeV and $g' \in \left[10^{-3}, 1\right]$, assuming annihilation to $\pi_d^0\pi_d^0$ dominates. The available parameter space is thus larger than for conventional WIMP dark matter, which CMB constraints [53] and Fermi dwarf galaxy observations [89] force to be heavier than $\mathcal{O}(10 \sim 100)\,$GeV. This is the main success of the Impeded Dark Matter paradigm.

IV. CONCLUSIONS

In summary, we have studied a class of dark matter models dubbed "Impeded DM", which are characterized by a very small mass splitting Δ between the DM and its annihilation products. Δ can be either positive or negative. For negative Δ, Impeded DM is characterized by an annihilation cross-section $\sigma v_{\rm rel}$ that grows *linearly* with $v_{\rm rel}$. This behavior allows for a regular thermal freeze-out, while constraints from low-$v_{\rm rel}$ environments (CMB, dwarf galaxies) are suppressed. For positive Δ, the annihilation cross-section can be suppressed by the small ratio $\Delta/m_{\rm DM}$.

We presented two specific models that realize the Impeded DM phenomenology (see table III for a summary of $\sigma v_{\rm rel}$ for the two models under different conditions). In the first one, DM comes in the form of massive gauge bosons associated with a dark sector $SU(2)_d$ group. When $SU(2)_d$ is broken, the mass of one of the three gauge bosons is changed by a small amount, typically upwards ($\Delta < 0$). The lighter gauge bosons constitute the DM, while the slightly heavier gauge boson interacts with the SM sector through a non-Abelian kinetic mixing term induced by a dimension six operator.

In the second Impeded DM model, the dark matter is composite. It features a confining gauge group $SU(N)$ and two species of dark quarks, which form dark pions. An additional $U(1)'$ (dark electromagnetism) splits the pion triplet in such a way that the DM particles $\pi_d^\pm$ are typically heavier than the neutral π_d^0, into which they annihilate. The dark and visible sectors are coupled through kinetic mixing of the dark and visible photons.

Model	$SU(2)_d$ dark gauge boson		dark pion
mass splitting	$\Delta \simeq -\frac{1}{2}\varepsilon^2 m_{\rm DM}$, eq. (10)		$\Delta \simeq g'^2 f_\pi^2/(2m_\pi)$, eq. (28)
	$10^{-7} \lesssim \varepsilon \lesssim 10^{-3}$	$\varepsilon \gtrsim 10^{-3}$	$g' \gtrsim 0.05$
	$\Delta < 0$ small	$\Delta < 0$ large	$\Delta > 0$
freeze-out	$\sigma v_{\rm rel} \propto v_{\rm rel}$		
CMB	$\sigma v_{\rm rel} \simeq 0$	$\sigma v_{\rm rel} \simeq 0$	$\sigma v_{\rm rel} \propto \sqrt{\frac{2\Delta}{m_{\rm DM}}}$
Galaxies	$\sigma v_{\rm rel} \propto v_{\rm rel}$		
Clusters			$\sigma v_{\rm rel} \propto \mathbf{BF} \times \sqrt{\frac{2\Delta}{m_{\rm DM}}}$

Table III. Mass splittings Δ and annihilation cross-sections $\sigma v_{\rm rel}$ for the two Impeded DM models discussed in this paper. In the $SU(2)_d$ dark gauge boson model, Δ depends on the kinetic mixing parameter ε, while in the dark pion model it depends on the $U(1)'$ (dark electromagnetic) gauge coupling g'. Note that the annihilation cross-section in galaxies clusters receives a boost factor (**BF**) from halo substructure in the dark pion model, while a similar boost is absent in the $SU(2)_d$ model as $\sigma v_{\rm rel}$ drops at small $v_{\rm rel}$.

For both models, we have presented detailed investigations of the phenomenology and have constrained the parameter space using all available data from cosmology, direct and indirect detection.

We conclude that Impeded DM populates a new niche in DM model space, but a niche that is becoming more and more interesting as CMB and dwarf galaxy constraints on DM annihilation put conventional thermal relic models under severe pressure.

ACKNOWLEDGMENTS

JK would like to thank Fermilab and the Aspen Center for Physics for hospitality and support during the final stages of this project, as well as Lufthansa for discounted WiFi access and a power outlet at a particularly critical time. WX is grateful to the Mainz Institute for Theoretical Physics (MITP) for its hospitality and its partial support during the completion of this work. JL and XPW would like to thank Yang Bai for helpful discussion. The work of JK, JL, and XPW is supported by the German Research Foundation (DFG) under Grant Nos. KO 4820/1–1 and FOR 2239 and by the European Research Council (ERC) under the European Union's Horizon 2020 research and innovation programme (grant agreement No. 637506, "νDirections"). The work of TS and WX is supported by the U.S. Department of Energy under grant Contract Numbers DE−SC00012567 and DE−SC0013999.

Appendix A: DM annihilation to SM particles in the $SU(2)_d$ model

We list here the annihilation cross-sections for the processes $K_1K_2 \to u\bar{u}, d\bar{d}, e^+e^-, \nu\bar{\nu}, W^+W^-$ in the $SU(2)_d$ model

$$\sigma v_{\rm rel}(K_1K_2 \to u\bar{u}) = \frac{e^2 g_d^2 v^2 \varepsilon^2 \sqrt{m_k^2 - m_u^2}}{3888\pi \cos^4\theta_w m_k^5 \left(4m_k^4 - 5m_k^2 m_Z^2 + m_Z^4\right)^2} \times \left\{64\cos^4\theta_w m_Z^8 \left(2m_k^2 + m_u^2\right)\right.$$
$$\left. - 32\cos^2\theta_w m_k^2 m_Z^6 (28\cos^2\theta_w - 5)(2m_k^2 + m_u^2) + 16 m_k^8 (68 m_k^2 + 7 m_u^2)\right.$$

$$
\begin{aligned}
&- 16m_k^6 m_Z^2 \left[4m_k^2(70\cos^2\theta_w - 17) + 7m_u^2(20\cos^2\theta_w - 1)\right] \\
&+ m_k^4 m_Z^4 \left[4\left(3008\cos^4\theta_w - 2200\cos^2\theta_w + 833\right)m_k^2\right. \\
&+ \left.\left(6016\cos^4\theta_w - 4400\cos^2\theta_w + 343\right)m_u^2\right] \Big\} \,, \qquad \text{(A1)}
\end{aligned}
$$

$$
\begin{aligned}
\sigma v_{\rm rel}(K_1K_2 \to d\bar{d}) = {} & \frac{e^2 g_d^2 v^2 \varepsilon^2 \sqrt{m_k^2 - m_d^2}}{3888\pi\cos^4\theta_w m_k^5 \left(4m_k^4 - 5m_k^2 m_Z^2 + m_Z^4\right)^2} \times \Big\{ 16\cos^4\theta_w m_Z^8 (2m_k^2 + m_d^2) \\
&- 16\cos^2\theta_w m_k^2 m_Z^6 \left(14\cos^2\theta_w - 1\right)\left(2m_k^2 + m_d^2\right) + 16m_k^8\left(20m_k^2 - 17m_d^2\right) \\
&- 16m_k^6 m_Z^2 \left[4m_k^2(7\cos^2\theta_w - 5) + m_d^2(14\cos^2\theta_w + 17)\right] \\
&+ m_k^4 m_Z^4 \left[4m_k^2\left(752\cos^4\theta_w - 220\cos^2\theta_w + 245\right)\right. \\
&+ \left. m_d^2\left(1504\cos^4\theta_w - 440\cos^2\theta_w - 833\right)\right] \Big\} \,, \qquad \text{(A2)}
\end{aligned}
$$

$$
\begin{aligned}
\sigma v_{\rm rel}(K_1K_2 \to e^+e^-) = {} & \frac{e^2 g_d^2 v^2 \varepsilon^2 \sqrt{m_k^2 - m_e^2}}{1296\pi\cos^4\theta_w m_k^5 \left(4m_k^4 - 5m_k^2 m_Z^2 + m_Z^4\right)^2} \times \Big\{ 16\cos^4\theta_w m_Z^8 (2m_k^2 + m_e^2) \\
&- 16\cos^2\theta_w m_k^2 m_Z^6 \left(14\cos^2\theta_w - 3\right)\left(2m_k^2 + m_e^2\right) + 16m_k^8\left(20m_k^2 + 7m_e^2\right) \\
&- 16m_k^6 m_Z^2 \left[4m_k^2(21\cos^2\theta_w - 5) + 7m_e^2(6\cos^2\theta_w - 1)\right] \\
&+ m_k^4 m_Z^4 \left[4m_k^2\left(752\cos^4\theta_w - 660\cos^2\theta_w + 245\right)\right. \\
&+ \left. m_e^2\left(1504\cos^4\theta_w - 1320\cos^2\theta_w + 343\right)\right] \Big\} \,, \qquad \text{(A3)}
\end{aligned}
$$

$$
\sigma v_{\rm rel}(K_1K_2 \to \nu\bar{\nu}) = \frac{e^2 g_d^2 v^2 \varepsilon^2 \sqrt{m_k^2 - m_\nu^2}\left(4m_k^2 - m_\nu^2\right)}{1296\pi\cos^4\theta_w m_k \left(4m_k^4 - 5m_k^2 m_Z^2 + m_Z^4\right)^2}\left(16m_k^2 + 16m_k^2 m_Z^2 + 49m_Z^4\right) \,, \qquad \text{(A4)}
$$

$$
\begin{aligned}
\sigma v_{\rm rel}(K_1K_2 \to W^+W^-) = {} & \frac{e^2 g_d^2 v^2 \varepsilon^2}{162\pi\cos^4\theta_w m_k^5 \left(4m_k^4 - 5m_k^2 m_Z^2 + m_Z^4\right)^2}\left(94m_k^4 - 14m_k^2 m_Z^2 + m_Z^4\right) \\
&\times \left(m_k^2 - \cos^2\theta_w m_Z^2\right)^{\frac{3}{2}}\left(3\cos^4\theta_w m_Z^4 + 20\cos^2\theta_w m_k^2 m_Z^2 + 4m_k^4\right) \,, \qquad \text{(A5)}
\end{aligned}
$$

where $v = v_{\rm rel}/2$. We see that all of these cross-sections are proportional to $v_{\rm rel}^2$, i.e. they are p-wave suppressed. Proportionality to ε^2 leads to an additional suppression.

The p-wave nature of K_1K_2 annihilation to SM particles can be understood by considering that all of the above processes involve the coupling $(K_1^\mu \partial_\mu K_2^\nu - K_2^\mu \partial_\mu K_1^\nu)$. In the non-relativistic limit, only contributions involving derivatives with respect to time could in principle be unsuppressed by $v_{\rm rel}^2$. These contributions have the form $m_k(\xi_1^0\xi_2^i - \xi_2^0\xi_1^i)$, where ξ^μ are the polarization vectors of the DM particles, and $i = 1, 2, 3$. This is a p-wave state [141], therefore the overall annihilation cross-section must be p-wave suppressed.

Appendix B: K_3 decay to SM particles in the $SU(2)_d$ model

The partial decay widths of K_3 for decays to SM particles are obtained from the non-Abelian kinetic mixing term eq. (6), after removing the mixing and rotating to mass eigenstates according to eq. (8). We find

$$
\begin{aligned}
\Gamma(K_3 \to u\bar{u}) = {} & \frac{\varepsilon^2 e^2 \sqrt{m_k^2 - 4m_u^2}}{288\pi\cos^4\theta_w m_k^2 (m_k^2 - m_Z^2)^2}\left[m_k^6(17 - 40\cos\theta_w + 72\cos^2\theta_w - 64\cos^3\theta_w + 32\cos^4\theta_w)\right. \\
&+ 64\cos^4\theta_w m_u^2 m_Z^4 - 16\cos^2\theta_w m_k^2 m_Z^2 (m_u^2(5 - 8\cos\theta_w + 8\cos^2\theta_w) - 2\cos^2\theta_w m_Z^2)
\end{aligned}
$$

$$+ m_k^4(m_u^2(7 - 80\cos\theta_w + 144\cos^2\theta_w - 128\cos^3\theta_w + 64\cos^4\theta_w)$$
$$-8\cos^2\theta_w m_Z^2(5 - 8\cos\theta_w + 8\cos^2\theta_w))\big] \,, \tag{B1}$$

$$\Gamma(K_3 \to d\bar{d}) = \frac{\varepsilon^2 e^2\sqrt{m_k^2 - 4m_d^2}}{288\pi\cos^4\theta_w m_k^2(m_k^2 - m_Z^2)^2}\big[m_k^6(5 - 4\cos\theta_w + 12\cos^2\theta_w - 16\cos^3\theta_w + 8\cos^4\theta_w)$$
$$- 4\cos^2\theta_w m_k^4 m_Z^2(1 - 2\cos\theta_w)^2 + 8\cos^4\theta_w m_k^2 m_Z^4$$
$$+ m_d^2(m_k^4(-17 - 8\cos\theta_w + 24\cos^2\theta_w - 32\cos^3\theta_w + 16\cos^4\theta_w)$$
$$-8\cos^2\theta_w m_k^2 m_Z^2(1 - 2\cos\theta_w)^2 + 16\cos^4\theta_w m_Z^4)\big] \,, \tag{B2}$$

$$\Gamma(K_3 \to e^+e^-) = \frac{\varepsilon^2 e^2\sqrt{m_k^2 - 4m_e^2}}{96\pi\cos^4\theta_w m_k^2(m_k^2 - m_Z^2)^2}\big[m_k^6(5 - 12\cos\theta_w + 20\cos^2\theta_w - 16\cos^3\theta_w + 8\cos^4\theta_w)$$
$$- 4\cos^2\theta_w m_k^4 m_Z^2(3 - 4\cos\theta_w + 4\cos^2\theta_w) + 8\cos^4\theta_w m_k^2 m_Z^4$$
$$+ m_e^2(m_k^4(7 - 24\cos\theta_w + 40\cos^2\theta_w - 32\cos^3\theta_w + 16\cos^4\theta_w)$$
$$- 8\cos^2\theta_w m_k^2 m_Z^2(3 - 4\cos\theta_w + 4\cos^2\theta_w) + 16\cos^4\theta_w m_Z^4)\,]\,, \tag{B3}$$

$$\Gamma(K_3 \to \nu\bar{\nu}) = \frac{\varepsilon^2 e^2 m_k^5}{96\pi\cos^4\theta_w(m_k^2 - m_Z^2)^2}\,, \tag{B4}$$

$$\Gamma(K_3 \to W^+W^-) = \frac{\varepsilon^2 e^2\sqrt{m_k^2 - 4\cos^2\theta_w m_Z^2}}{192\pi\cos^4\theta_w m_k^2(m_k^2 - m_Z^2)^2}$$
$$\times\left(m_k^6 + 16\cos^2\theta_w m_k^4 m_Z^2 - 68\cos^4\theta_w m_k^2 m_Z^4 - 48\cos^6\theta_w m_Z^6\right)\,. \tag{B5}$$

[1] M. Pospelov, A. Ritz, and M. B. Voloshin, "Secluded WIMP Dark Matter," *Phys. Lett.* **B662** (2008) 53–61, arXiv:0711.4866 [hep-ph].

[2] N. Arkani-Hamed, D. P. Finkbeiner, T. R. Slatyer, and N. Weiner, "A Theory of Dark Matter," *Phys. Rev.* **D79** (2009) 015014, arXiv:0810.0713 [hep-ph].

[3] Y. Hochberg, E. Kuflik, T. Volansky, and J. G. Wacker, "Mechanism for Thermal Relic Dark Matter of Strongly Interacting Massive Particles," *Phys. Rev. Lett.* **113** (2014) 171301, arXiv:1402.5143 [hep-ph].

[4] Y. Hochberg, E. Kuflik, H. Murayama, T. Volansky, and J. G. Wacker, "Model for Thermal Relic Dark Matter of Strongly Interacting Massive Particles," *Phys. Rev. Lett.* **115** no. 2, (2015) 021301, arXiv:1411.3727 [hep-ph].

[5] H. M. Lee and M.-S. Seo, "Communication with SIMP dark mesons via Z -portal," *Phys. Lett.* **B748** (2015) 316–322, arXiv:1504.00745 [hep-ph].

[6] Y. Hochberg, E. Kuflik, and H. Murayama, "SIMP Spectroscopy," *JHEP* **05** (2016) 090, arXiv:1512.07917 [hep-ph].

[7] R. T. D'Agnolo and A. Hook, "Selfish Dark Matter," *Phys. Rev.* **D91** no. 11, (2015) 115020, arXiv:1504.00361 [hep-ph].

[8] R. T. D'Agnolo and J. T. Ruderman, "Light Dark Matter from Forbidden Channels," *Phys. Rev. Lett.* **115** no. 6, (2015) 061301, arXiv:1505.07107 [hep-ph].

[9] A. Delgado, A. Martin, and N. Raj, "Forbidden Dark Matter at the Weak Scale via the Top Portal," arXiv:1608.05345 [hep-ph].

[10] E. D. Carlson, M. E. Machacek, and L. J. Hall, "Self-Interacting Dark Matter," *Astrophys. J.* **398** (1992) 43–52.

[11] D. Pappadopulo, J. T. Ruderman, and G. Trevisan, "Dark matter freeze-out in a nonrelativistic sector," *Phys. Rev.* **D94** no. 3, (2016) 035005, arXiv:1602.04219 [hep-ph].

[12] N. Bernal, X. Chu, C. Garcia-Cely, T. Hambye, and B. Zaldivar, "Production Regimes for Self-Interacting Dark Matter," *JCAP* **1603** no. 03, (2016) 018, arXiv:1510.08063 [hep-ph].

[13] E. Kuflik, M. Perelstein, N. R.-L. Lorier, and Y.-D. Tsai, "Elastically Decoupling Dark Matter," *Phys. Rev. Lett.* **116** no. 22, (2016) 221302, arXiv:1512.04545 [hep-ph].

[14] N. Bernal and X. Chu, "Z_2 SIMP Dark Matter," *JCAP* **1601** (2016) 006, arXiv:1510.08527 [hep-ph].

[15] M. Farina, D. Pappadopulo, J. T. Ruderman, and G. Trevisan, "Phases of Cannibal Dark Matter," arXiv:1607.03108 [hep-ph].

[16] J. A. Dror, E. Kuflik, and W. H. Ng, "Co-Decaying Dark Matter," arXiv:1607.03110 [hep-ph].

[17] S. Okawa, M. Tanabashi, and M. Yamanaka, "Relic Abundance in Secluded Dark Matter Scenario with Massive Mediator," arXiv:1607.08520 [hep-ph].

[18] P. Bandyopadhyay, E. J. Chun, and J.-C. Park, "Right-handed sneutrino dark matter in $\mathbf{U}(\mathbf{1})'$ seesaw models and its signatures at the LHC," *JHEP* **06** (2011) 129, arXiv:1105.1652 [hep-ph].

[19] F. D'Eramo and J. Thaler, "Semi-annihilation of Dark Matter," *JHEP* **06** (2010) 109, arXiv:1003.5912 [hep-ph].

[20] K. Agashe, Y. Cui, L. Necib, and J. Thaler, "(In)Direct Detection of Boosted Dark Matter," *JCAP* **1410** no. 10, (2014) 062, arXiv:1405.7370 [hep-ph].

[21] J. Berger, Y. Cui, and Y. Zhao, "Detecting Boosted Dark Matter from the Sun with Large Volume Neutrino Detectors," *JCAP* **1502** no. 02, (2015) 005, arXiv:1410.2246 [hep-ph].

[22] J. Kopp, J. Liu, and X.-P. Wang, "Boosted Dark Matter in IceCube and at the Galactic Center," *JHEP* **04** (2015) 105, arXiv:1503.02669 [hep-ph].

[23] A. Berlin, D. Hooper, and G. Krnjaic, "Pev-Scale Dark Matter as a Thermal Relic of a Decoupled Sector," *Phys. Lett.* **B760** (2016) 106–111, arXiv:1602.08490 [hep-ph].

[24] L.-B. Jia, "Study of WIMP annihilations into a pair of on-shell scalar mediators," arXiv:1607.00737 [hep-ph].

[25] J. Fan, M. Reece, and J. T. Ruderman, "Stealth Supersymmetry," *JHEP* **11** (2011) 012, arXiv:1105.5135 [hep-ph].

[26] J. Fan, M. Reece, and J. T. Ruderman, "A Stealth Supersymmetry Sampler," *JHEP* **07** (2012) 196, arXiv:1201.4875 [hep-ph].

[27] J. Fan, R. Krall, D. Pinner, M. Reece, and J. T. Ruderman, "Stealth Supersymmetry Simplified," *JHEP* **07** (2016) 016, arXiv:1512.05781 [hep-ph].

[28] T. Hambye, "Hidden Vector Dark Matter," *JHEP* **01** (2009) 028, arXiv:0811.0172 [hep-ph].

[29] T. Hambye and M. H. G. Tytgat, "Confined hidden vector dark matter," *Phys. Lett.* **B683** (2010) 39–41, arXiv:0907.1007 [hep-ph].

[30] Y. Farzan and A. R. Akbarieh, "VDM: A model for Vector Dark Matter," *JCAP* **1210** (2012) 026, arXiv:1207.4272 [hep-ph].

[31] S. Baek, P. Ko, W.-I. Park, and E. Senaha, "Higgs Portal Vector Dark Matter : Revisited," *JHEP* **05** (2013) 036, arXiv:1212.2131 [hep-ph].

[32] S. Baek, P. Ko, and W.-I. Park, "Hidden sector monopole, vector dark matter and dark radiation with Higgs portal," *JCAP* **1410** no. 10, (2014) 067, arXiv:1311.1035 [hep-ph].

[33] P. Ko, W.-I. Park, and Y. Tang, "Higgs portal vector dark matter for GeV scale γ-ray excess from galactic center," *JCAP* **1409** (2014) 013, arXiv:1404.5257 [hep-ph].

[34] S. Baek, P. Ko, W.-I. Park, and Y. Tang, "Indirect and direct signatures of Higgs portal decaying vector dark matter for positron excess in cosmic rays," *JCAP* **1406** (2014) 046, arXiv:1402.2115 [hep-ph].

[35] S. Baek, P. Ko, and W.-I. Park, "Invisible Higgs Decay Width vs. Dark Matter Direct Detection Cross Section in Higgs Portal Dark Matter Models," *Phys. Rev.* **D90** no. 5, (2014) 055014, arXiv:1405.3530 [hep-ph].

[36] C.-H. Chen and T. Nomura, "$SU(2)_X$ vector DM and Galactic Center gamma-ray excess," *Phys. Lett.* **B746** (2015) 351–358, arXiv:1501.07413 [hep-ph].

[37] C. Gross, O. Lebedev, and Y. Mambrini, "Non-Abelian gauge fields as dark matter," *JHEP* **08** (2015) 158, arXiv:1505.07480 [hep-ph].

[38] J. S. Kim, O. Lebedev, and D. Schmeier, "Higgsophilic gauge bosons and monojets at the LHC," *JHEP* **11** (2015) 128, arXiv:1507.08673 [hep-ph].

[39] S. Di Chiara and K. Tuominen, "A minimal model for SU(N) vector dark matter," *JHEP* **11** (2015) 188, arXiv:1506.03285 [hep-ph].

[40] C.-H. Chen and T. Nomura, "Searching for vector dark matter via Higgs portal at the LHC," *Phys. Rev.* **D93** no. 7, (2016) 074019, arXiv:1507.00886 [hep-ph].

[41] A. Karam and K. Tamvakis, "Dark Matter from a Classically Scale-Invariant $SU(3)_X$," arXiv:1607.01001 [hep-ph].

[42] J. L. Diaz-Cruz and E. Ma, "Neutral SU(2) Gauge Extension of the Standard Model and a Vector-Boson Dark-Matter Candidate," *Phys. Lett.* **B695** (2011) 264–267, arXiv:1007.2631 [hep-ph].

[43] S. Bhattacharya, J. L. Diaz-Cruz, E. Ma, and D. Wegman, "Dark Vector-Gauge-Boson Model," *Phys. Rev.* **D85** (2012) 055008, arXiv:1107.2093 [hep-ph].

[44] C.-W. Chiang, T. Nomura, and J. Tandean, "Nonabelian Dark Matter with Resonant Annihilation," *JHEP* **01** (2014) 183, arXiv:1306.0882 [hep-ph].

[45] S. Fraser, E. Ma, and M. Zakeri, "$SU(2)_N$ model of vector dark matter with a leptonic connection," *Int. J. Mod. Phys.* **A30** no. 03, (2015) 1550018, arXiv:1409.1162 [hep-ph].

[46] H. Davoudiasl and I. M. Lewis, "Dark Matter from Hidden Forces," *Phys. Rev.* **D89** no. 5, (2014) 055026, arXiv:1309.6640 [hep-ph].

[47] A. DiFranzo, P. J. Fox, and T. M. P. Tait, "Vector Dark Matter through a Radiative Higgs Portal," *JHEP* **04** (2016) 135, arXiv:1512.06853 [hep-ph].

[48] F. D'Eramo, M. McCullough, and J. Thaler, "Multiple Gamma Lines from Semi-Annihilation," *JCAP* **1304** (2013) 030, arXiv:1210.7817 [hep-ph].

[49] P. Gondolo and G. Gelmini, "Cosmic Abundances of Stable Particles: Improved Analysis," *Nucl. Phys.* **B360** (1991) 145–179.

[50] the LUX collaboration, "Dark-matter results from 332 new live days of lux data." http://luxdarkmatter.org/LUX_dark_matter/Talks_files/LUX_NewDarkMatterSearchResult_332LiveDays_IDM2016_160721.pdf. talk at the 11th Identification of Dark Matter conference.

[51] **LUX** Collaboration, D. S. Akerib *et al.*, "Improved Limits on Scattering of Weakly Interacting Massive Particles from Reanalysis of 2013 Lux Data," *Phys. Rev. Lett.* **116** no. 16, (2016) 161301, arXiv:1512.03506 [astro-ph.CO].

[52] **PandaX-II** Collaboration, A. Tan *et al.*, "Dark Matter Results from First 98.7-day Data of PandaX-II Experiment," arXiv:1607.07400 [hep-ex].

[53] **Planck** Collaboration, P. A. R. Ade *et al.*, "Planck 2015 results. XIII. Cosmological parameters," arXiv:1502.01589 [astro-ph.CO].

[54] **Fermi-LAT** Collaboration, M. Ackermann *et al.*, "Search for Gamma-Ray Spectral Lines with the Fermi Large Area Telescope and Dark Matter Implications," *Phys. Rev.* **D88** (2013) 082002, arXiv:1305.5597 [astro-ph.HE].

[55] G. Ovanesyan, T. R. Slatyer, and I. W. Stewart, "Heavy Dark Matter Annihilation from Effective Field Theory," *Phys. Rev. Lett.* **114** no. 21, (2015) 211302, arXiv:1409.8294 [hep-ph].

[56] J. M. Cline, G. Dupuis, Z. Liu, and W. Xue, "The Windows for Kinetically Mixed Z'-Mediated Dark Matter and the Galactic Center Gamma Ray Excess," *JHEP* **08** (2014) 131, arXiv:1405.7691 [hep-ph].

[57] A. Hook, E. Izaguirre, and J. G. Wacker, "Model Independent Bounds on Kinetic Mixing," *Adv. High Energy Phys.* **2011** (2011) 859762, arXiv:1006.0973 [hep-ph].

[58] **CHARM** Collaboration, F. Bergsma *et al.*, "A Search for Decays of Heavy Neutrinos in the Mass Range 0.5-GeV to 2.8-GeV," *Phys. Lett.* **B166** (1986) 473.

[59] A. Konaka *et al.*, "Search for Neutral Particles in Electron Beam Dump Experiment," *Phys. Rev. Lett.* **57** (1986) 659.

[60] E. M. Riordan *et al.*, "A Search for Short Lived Axions in an Electron Beam Dump Experiment," *Phys. Rev. Lett.* **59** (1987) 755.

[61] J. D. Bjorken, S. Ecklund, W. R. Nelson, A. Abashian, C. Church, B. Lu, L. W. Mo, T. A. Nunamaker, and P. Rassmann, "Search for Neutral Metastable Penetrating Particles Produced in the SLAC Beam Dump," *Phys. Rev.* **D38** (1988) 3375.

[62] A. Bross, M. Crisler, S. H. Pordes, J. Volk, S. Errede, and J. Wrbanek, "A Search for Shortlived Particles Produced in an Electron Beam Dump," *Phys. Rev. Lett.* **67** (1991) 2942–2945.

[63] M. Davier and H. Nguyen Ngoc, "An Unambiguous Search for a Light Higgs Boson," *Phys. Lett.* **B229** (1989) 150.

[64] **LSND** Collaboration, C. Athanassopoulos *et al.*, "Evidence for muon-neutrino —¿ electron-neutrino oscillations from pion decay in flight neutrinos," *Phys. Rev.* **C58** (1998) 2489–2511, arXiv:nucl-ex/9706006 [nucl-ex].

[65] **NOMAD collaboration** Collaboration, P. Astier *et al.*, "Search for heavy neutrinos mixing with tau neutrinos," *Phys. Lett.* **B506** (2001) 27–38, arXiv:hep-ex/0101041 [hep-ex].

[66] **E787** Collaboration, S. Adler *et al.*, "Further search for the decay K+ —¿ pi+ nu anti-nu in the momentum region P ¡ 195-MeV/c," *Phys. Rev.* **D70** (2004) 037102, arXiv:hep-ex/0403034 [hep-ex].

[67] J. D. Bjorken, R. Essig, P. Schuster, and N. Toro, "New Fixed-Target Experiments to Search for Dark Gauge Forces," *Phys. Rev.* **D80** (2009) 075018, arXiv:0906.0580 [hep-ph].

[68] **BNL-E949** Collaboration, A. V. Artamonov *et al.*, "Study of the decay K+ —¿ pi+ nu anti-nu in the momentum region 140 ¡ P(pi) ¡ 199-MeV/c," *Phys. Rev.* **D79** (2009) 092004, arXiv:0903.0030 [hep-ex].

[69] R. Essig, R. Harnik, J. Kaplan, and N. Toro, "Discovering New Light States at Neutrino Experiments," *Phys. Rev.* **D82** (2010) 113008, arXiv:1008.0636 [hep-ph].

[70] J. Blumlein and J. Brunner, "New Exclusion Limits for Dark Gauge Forces from Beam-Dump Data," *Phys. Lett.* **B701** (2011) 155–159, arXiv:1104.2747 [hep-ex].

[71] S. Gninenko, "Constraints on sub-GeV hidden sector gauge bosons from a search for heavy neutrino decays," *Phys. Lett.* **B713** (2012) 244–248, arXiv:1204.3583 [hep-ph].

[72] J. Blmlein and J. Brunner, "New Exclusion Limits on Dark Gauge Forces from Proton Bremsstrahlung in Beam-Dump Data," *Phys. Lett.* **B731** (2014) 320–326, arXiv:1311.3870 [hep-ph].

[73] **APEX collaboration** Collaboration, S. Abrahamyan *et al.*, "Search for a New Gauge Boson in Electron-Nucleus Fixed-Target Scattering by the APEX Experiment," *Phys. Rev. Lett.* **107** (2011) 191804, arXiv:1108.2750 [hep-ex].

[74] H. Merkel *et al.*, "Search at the Mainz Microtron for Light Massive Gauge Bosons Relevant for the Muon g-2 Anomaly," *Phys. Rev. Lett.* **112** no. 22, (2014) 221802, arXiv:1404.5502 [hep-ex].

[75] **A1** Collaboration, H. Merkel *et al.*, "Search for Light Gauge Bosons of the Dark Sector at the Mainz Microtron," *Phys. Rev. Lett.* **106** (2011) 251802, arXiv:1101.4091 [nucl-ex].

[76] **BaBar** Collaboration, B. Aubert *et al.*, "Search for Dimuon Decays of a Light Scalar Boson in Radiative Transitions Upsilon —¿ gamma A0," *Phys. Rev. Lett.* **103** (2009) 081803, arXiv:0905.4539 [hep-ex].

[77] D. Curtin *et al.*, "Exotic decays of the 125 GeV Higgs boson," *Phys. Rev.* **D90** no. 7, (2014) 075004, arXiv:1312.4992 [hep-ph].

[78] **BaBar** Collaboration, J. P. Lees *et al.*, "Search for a Dark Photon in e^+e^- Collisions at BaBar," *Phys. Rev. Lett.* **113** no. 20, (2014) 201801, arXiv:1406.2980 [hep-ex].

[79] G. Bernardi, G. Carugno, J. Chauveau, F. Dicarlo, M. Dris, *et al.*, "Search for Neutrino Decay," *Phys. Lett.* **B166** (1986) 479.

[80] **SINDRUM I collaboration** Collaboration, R. Meijer Drees *et al.*, "Search for weakly interacting neutral bosons produced in pi- p interactions at rest and decaying into e+ e- pairs.," *Phys. Rev. Lett.* **68** (1992) 3845–3848.

[81] **KLOE-2 collaboration** Collaboration, F. Archilli *et al.*, "Search for a vector gauge boson in phi meson decays with the KLOE detector," *Phys. Lett.* **B706** (2012) 251–255, arXiv:1110.0411 [hep-ex].

[82] S. N. Gninenko, "Stringent limits on the $\pi^0 -> \gamma X, X -> e + e-$ decay from neutrino experiments and constraints on new light gauge bosons," *Phys. Rev.* **D85** (2012) 055027, arXiv:1112.5438 [hep-ph].

[83] **KLOE-2 collaboration** Collaboration, D. Babusci *et al.*, "Limit on the production of a light vector gauge boson in phi meson decays with the KLOE detector," *Phys. Lett.* **B720** (2013) 111–115, arXiv:1210.3927 [hep-ex].

[84] **WASA-at-COSY collaboration** Collaboration, P. Adlarson *et al.*, "Search for a dark photon in the $\pi^0 \to e^+e^-\gamma$ decay," *Phys. Lett.* **B726** (2013) 187–193, arXiv:1304.0671 [hep-ex].

[85] **HADES collaboration** Collaboration, G. Agakishiev *et al.*, "Searching a Dark Photon with HADES," *Phys. Lett.* **B731** (2014) 265–271, arXiv:1311.0216 [hep-ex].

[86] **PHENIX collaboration** Collaboration, A. Adare *et al.*, "Search for dark photons from neutral meson decays in $p+p$ and d + Au collisions at $\sqrt{s_{NN}} = 200$ GeV," *Phys. Rev.* **C91** no. 3, (2015) 031901, arXiv:1409.0851 [nucl-ex].

[87] **NA48/2** Collaboration, J. R. Batley *et al.*, "Search for the dark photon in π^0 decays," *Phys. Lett.* **B746** (2015) 178–185, arXiv:1504.00607 [hep-ex].

[88] **KLOE-2** Collaboration, A. Anastasi *et al.*, "Limit on the production of a new vector boson in $e^+e^- \to U\gamma$, $U \to \pi^+\pi^-$ with the KLOE experiment," arXiv:1603.06086 [hep-ex].

[89] **Fermi-LAT** Collaboration, M. Ackermann *et al.*, "Searching for Dark Matter Annihilation from MilkyWay Dwarf Spheroidal Galaxies with Six Years of Fermi Large Area Telescope Data," *Phys. Rev. Lett.* **115** no. 23, (2015) 231301, arXiv:1503.02641 [astro-ph.HE].

[90] G. Elor, N. L. Rodd, T. R. Slatyer, and W. Xue, "Model-Independent Indirect Detection Constraints on Hidden Sector Dark Matter," *JCAP* **1606** no. 06, (2016) 024, arXiv:1511.08787 [hep-ph].

[91] **Fermi-LAT** Collaboration, M. Ackermann *et al.*, "Search for Extended Gamma-Ray Emission from the Virgo Galaxy Cluster with Fermi-Lat," *Astrophys. J.* **812** no. 2, (2015) 159, arXiv:1510.00004 [astro-ph.HE].

[92] A. Massari, E. Izaguirre, R. Essig, A. Albert, E. Bloom, and G. A. Gmez-Vargas, "Strong Optimized Conservative *Fermi*-LAT Constraints on Dark Matter Models from the Inclusive Photon Spectrum," *Phys. Rev.* **D91** no. 8, (2015) 083539, arXiv:1503.07169 [hep-ph].

[93] R. Essig, E. Kuflik, S. D. McDermott, T. Volansky, and K. M. Zurek, "Constraining Light Dark Matter with Diffuse X-Ray and Gamma-Ray Observations," *JHEP* **11** (2013) 193, arXiv:1309.4091 [hep-ph].

[94] G. Jungman, M. Kamionkowski, and K. Griest, "Supersymmetric Dark Matter," *Phys. Rept.* **267** (1996) 195–373, arXiv:hep-ph/9506380 [hep-ph].

[95] E. Masso, S. Mohanty, and S. Rao, "Dipolar Dark Matter," *Phys. Rev.* **D80** (2009) 036009, arXiv:0906.1979 [hep-ph].

[96] E. Del Nobile, C. Kouvaris, P. Panci, F. Sannino, and J. Virkajarvi, "Light Magnetic Dark Matter in Direct Detection Searches," *JCAP* **1208** (2012) 010, arXiv:1203.6652 [hep-ph].

[97] D. S. Akerib *et al.*, "Results from a search for dark matter in LUX with 332 live days of exposure," arXiv:1608.07648 [astro-ph.CO].

[98] J. A. Adams, S. Sarkar, and D. Sciama, "CMB anisotropy in the decaying neutrino cosmology," *Mon.Not.Roy.Astron.Soc.* **301** (1998) 210–214, arXiv:astro-ph/9805108 [astro-ph].

[99] N. Padmanabhan and D. P. Finkbeiner, "Detecting Dark Matter Annihilation with CMB Polarization : Signatures and Experimental Prospects," *Phys. Rev.* **D72** (2005) 023508, astro-ph/0503486.

[100] S. Galli, F. Iocco, G. Bertone, and A. Melchiorri, "CMB constraints on Dark Matter models with large annihilation cross-section," *Phys. Rev.* **D80** (2009) 023505, arXiv:0905.0003 [astro-ph.CO].

[101] T. R. Slatyer, N. Padmanabhan, and D. P. Finkbeiner, "CMB Constraints on WIMP Annihilation: Energy Absorption During the Recombination Epoch," *Phys. Rev.* **D80** (2009) 043526, arXiv:0906.1197 [astro-ph.CO].

[102] D. P. Finkbeiner, S. Galli, T. Lin, and T. R. Slatyer, "Searching for Dark Matter in the CMB: A Compact Parameterization of Energy Injection from New Physics," *Phys. Rev.* **D85** (2012) 043522, arXiv:1109.6322 [astro-ph.CO].

[103] M. S. Madhavacheril, N. Sehgal, and T. R. Slatyer, "Current Dark Matter Annihilation Constraints from Cmb and Low-Redshift Data," *Phys. Rev.* **D89** (2014) 103508, arXiv:1310.3815 [astro-ph.CO].

[104] T. R. Slatyer, "Indirect dark matter signatures in the cosmic dark ages. I. Generalizing the bound on s-wave dark matter annihilation from Planck results," *Phys. Rev.* **D93** no. 2, (2016) 023527, arXiv:1506.03811 [hep-ph].

[105] J. Liu, N. Weiner, and W. Xue, "Signals of a Light Dark Force in the Galactic Center," *JHEP* **08** (2015) 050, arXiv:1412.1485 [hep-ph].

[106] F. Iocco, M. Pato, G. Bertone, and P. Jetzer, "Dark Matter distribution in the Milky Way: microlensing and dynamical constraints," *JCAP* **1111** (2011) 029, arXiv:1107.5810 [astro-ph.GA].

[107] R. Catena and P. Ullio, "A novel determination of the local dark matter density," *JCAP* **1008** (2010) 004, arXiv:0907.0018 [astro-ph.CO].

[108] P. Salucci, F. Nesti, G. Gentile, and C. F. Martins, "The dark matter density at the Sun's location," *Astron. Astrophys.* **523** (2010) A83, arXiv:1003.3101 [astro-ph.GA].

[109] M. Cirelli, G. Corcella, A. Hektor, G. Hutsi, M. Kadastik, P. Panci, M. Raidal, F. Sala, and A. Strumia, "PPpc 4 Dm Id: a Poor Particle Physicist Cookbook for Dark Matter Indirect Detection," *JCAP* **1103** (2011) 051, arXiv:1012.4515 [hep-ph]. [Erratum: JCAP1210,E01(2012)].

[110] F. Iocco, M. Pato, and G. Bertone, "Evidence for dark matter in the inner Milky Way," *Nature Phys.* **11** (2015) 245–248, arXiv:1502.03821 [astro-ph.GA].

[111] D. E. Gruber, J. L. Matteson, L. E. Peterson, and G. V. Jung, "The spectrum of diffuse cosmic hard x-rays measured with heao-1," *Astrophys. J.* **520** (1999) 124, arXiv:astro-ph/9903492 [astro-ph].

[112] L. Bouchet, E. Jourdain, J. P. Roques, A. Strong, R. Diehl, F. Lebrun, and R. Terrier, "INTEGRAL SPI All-Sky View in Soft Gamma Rays: Study of Point Source and Galactic Diffuse Emissions," *Astrophys. J.* **679** (2008) 1315, arXiv:0801.2086 [astro-ph].

[113] S. C. Kappadath, *Measurement of the Cosmic Diffuse Gamma-Ray Spectrum from 800 keV to 30 MeV*. PhD thesis, University of New Hampshire, USA, 1998.

[114] A. W. Strong, I. V. Moskalenko, and O. Reimer, "Diffuse galactic continuum gamma rays. A Model compatible with EGRET data and cosmic-ray measurements," *Astrophys. J.* **613** (2004) 962–976, arXiv:astro-ph/0406254 [astro-ph].

[115] **Fermi-LAT** Collaboration, M. Ackermann *et al.*, "Fermi-LAT Observations of the Diffuse Gamma-Ray Emission: Implications for Cosmic Rays and the Interstellar Medium," *Astrophys. J.* **750** (2012) 3, arXiv:1202.4039 [astro-ph.HE].

[116] **AMS** Collaboration, M. Aguilar *et al.*, "Electron and Positron Fluxes in Primary Cosmic Rays Measured with the Alpha Magnetic Spectrometer on the International Space Station," *Phys. Rev. Lett.* **113** (2014) 121102.

[117] L. Bergstrom, T. Bringmann, I. Cholis, D. Hooper, and C. Weniger, "New limits on dark matter annihilation from AMS cosmic ray positron data," *Phys. Rev. Lett.* **111** (2013) 171101, arXiv:1306.3983 [astro-ph.HE].

[118] C. Evoli, D. Gaggero, D. Grasso, and L. Maccione, "Cosmic-Ray Nuclei, Antiprotons and Gamma-Rays in the Galaxy: a New Diffusion Model," *JCAP* **0810** (2008) 018, arXiv:0807.4730 [astro-ph].

[119] L. Maccione, C. Evoli, D. Gaggero, and D. Grasso, "DRAGON: Galactic Cosmic Ray Diffusion Code." Astrophysics source code library, June, 2011.

[120] **H.E.S.S.** Collaboration, A. Abramowski *et al.*, "Search for Photon-Linelike Signatures from Dark Matter Annihilations with H.E.S.S.," *Phys. Rev. Lett.* **110** (2013) 041301, arXiv:1301.1173 [astro-ph.HE].

[121] S. Profumo, F. S. Queiroz, and C. E. Yaguna, "Extending Fermi-LAT and H.E.S.S. Limits on Gamma-ray Lines from Dark Matter Annihilation," arXiv:1602.08501 [astro-ph.HE].

[122] T. A. Ryttov and F. Sannino, "Ultra Minimal Technicolor and its Dark Matter TIMP," *Phys. Rev.* **D78** (2008) 115010, arXiv:0809.0713 [hep-ph].

[123] Y. Bai and A. Martin, "Topological Pions," *Phys. Lett.* **B693** (2010) 292–295, arXiv:1003.3006 [hep-ph].

[124] Y. Bai and R. J. Hill, "Weakly Interacting Stable Pions," *Phys. Rev.* **D82** (2010) 111701, arXiv:1005.0008 [hep-ph].

[125] T. Hur and P. Ko, "Scale invariant extension of the standard model with strongly interacting hidden sector," *Phys. Rev. Lett.* **106** (2011) 141802, arXiv:1103.2571 [hep-ph].

[126] J. Fan and M. Reece, "Simple dark matter recipe for the 111 and 128 GeV Fermi-LAT lines," *Phys. Rev.* **D88** no. 3, (2013) 035014, arXiv:1209.1097 [hep-ph].

[127] M. Frigerio, A. Pomarol, F. Riva, and A. Urbano, "Composite Scalar Dark Matter," *JHEP* **07** (2012) 015, arXiv:1204.2808 [hep-ph].

[128] M. R. Buckley and E. T. Neil, "Thermal dark matter from a confining sector," *Phys. Rev.* **D87** no. 4, (2013) 043510, arXiv:1209.6054 [hep-ph].
[129] S. Bhattacharya, B. Meli?, and J. Wudka, "Pionic Dark Matter," *JHEP* **02** (2014) 115, arXiv:1307.2647 [hep-ph].
[130] M. Holthausen, J. Kubo, K. S. Lim, and M. Lindner, "Electroweak and Conformal Symmetry Breaking by a Strongly Coupled Hidden Sector," *JHEP* **12** (2013) 076, arXiv:1310.4423 [hep-ph].
[131] J. M. Cline, Z. Liu, G. Moore, and W. Xue, "Composite strongly interacting dark matter," *Phys. Rev.* **D90** no. 1, (2014) 015023, arXiv:1312.3325 [hep-ph].
[132] N. Yamanaka, S. Fujibayashi, S. Gongyo, and H. Iida, "Dark matter in the hidden gauge theory," arXiv:1411.2172 [hep-ph].
[133] A. Carmona and M. Chala, "Composite Dark Sectors," *JHEP* **06** (2015) 105, arXiv:1504.00332 [hep-ph].
[134] Y. Ametani, M. Aoki, H. Goto, and J. Kubo, "Nambu-Goldstone Dark Matter in a Scale Invariant Bright Hidden Sector," *Phys. Rev.* **D91** no. 11, (2015) 115007, arXiv:1505.00128 [hep-ph].
[135] H. Hatanaka, D.-W. Jung, and P. Ko, "AdS/QCD approach to the scale-invariant extension of the standard model with a strongly interacting hidden sector," *JHEP* **08** (2016) 094, arXiv:1606.02969 [hep-ph].
[136] K. Harigaya and Y. Nomura, "Composite Models for the 750 GeV Diphoton Excess," *Phys. Lett.* **B754** (2016) 151–156, arXiv:1512.04850 [hep-ph].
[137] Y. Bai, J. Berger, and R. Lu, "750 GeV dark pion: Cousin of a dark G -parity odd WIMP," *Phys. Rev.* **D93** no. 7, (2016) 076009, arXiv:1512.05779 [hep-ph].
[138] T. Das, G. S. Guralnik, V. S. Mathur, F. E. Low, and J. E. Young, "Electromagnetic Mass Difference of Pions," *Phys. Rev. Lett.* **18** (1967) 759–761.
[139] J. F. Donoghue and A. F. Perez, "The Electromagnetic Mass Differences of Pions and Kaons," *Phys. Rev.* **D55** (1997) 7075–7092, arXiv:hep-ph/9611331 [hep-ph].
[140] S. Weinberg, "Pion Scattering Lengths," *Phys. Rev. Lett.* **17** (1966) 616–621.
[141] J. Kumar and D. Marfatia, "Matrix Element Analyses of Dark Matter Scattering and Annihilation," *Phys. Rev.* **D88** no. 1, (2013) 014035, arXiv:1305.1611 [hep-ph].